Response of Organ Structure and Physiology to Autotetraploidization in Early Development of Energy Willow *Salix viminalis*[1]

Dénes Dudits*, Katalin Török, András Cseri, Kenny Paul, Anna V. Nagy, Bettina Nagy, László Sass, Györgyi Ferenc, Radomira Vankova, Petre Dobrev, Imre Vass, and Ferhan Ayaydin

Institute of Plant Biology, Biological Research Centre, Hungarian Academy of Sciences, 6726 Szeged, Hungary (D.D., K.T., A.C., K.P., A.V.N., B.N., L.S., G.F., I.V., F.A.); and Institute of Experimental Botany, Academy of Sciences of the Czech Republic, Prague, Czech Republic (R.V., P.D.)

ORCID ID: 0000-0001-7980-4025 (A.V.N.).

The biomass productivity of the energy willow *Salix viminalis* as a short-rotation woody crop depends on organ structure and functions that are under the control of genome size. Colchicine treatment of axillary buds resulted in a set of autotetraploid *S. viminalis* var. Energo genotypes (polyploid Energo [PP-E]; $2n = 4x = 76$) with variation in the green pixel-based shoot surface area. In cases where increased shoot biomass was observed, it was primarily derived from larger leaf size and wider stem diameter. Autotetraploidy slowed primary growth and increased shoot diameter (a parameter of secondary growth). The duplicated genome size enlarged bark and wood layers in twigs sampled in the field. The PP-E plants developed wider leaves with thicker midrib and enlarged palisade parenchyma cells. Autotetraploid leaves contained significantly increased amounts of active gibberellins, cytokinins, salicylic acid, and jasmonate compared with diploid individuals. Greater net photosynthetic CO_2 uptake was detected in leaves of PP-E plants with increased chlorophyll and carotenoid contents. Improved photosynthetic functions in tetraploids were also shown by more efficient electron transport rates of photosystems I and II. Autotetraploidization increased the biomass of the root system of PP-E plants relative to diploids. Sections of tetraploid roots showed thickening with enlarged cortex cells. Elevated amounts of indole acetic acid, active cytokinins, active gibberellin, and salicylic acid were detected in the root tips of these plants. The presented variation in traits of tetraploid willow genotypes provides a basis to use autopolyploidization as a chromosome engineering technique to alter the organ development of energy plants in order to improve biomass productivity.

Energy security and climate change as global problems urge increased efforts to use plants as renewable energy sources both for power generation and transportation fuel production. Selected wood species, such as willows (*Salix* spp.), can be cultivated as short-rotation coppice for the rapid accumulation of biomass and reduction of CO_2 emission. Coppicing reinvigorates shoot growth, resulting in a special woody plant life cycle that differs from natural tree development, which takes decades. In this cultivation system, small stem cuttings are planted at high densities (15,000–25,000 ha^{-1}). In the soil, these dormant wood cuttings first produce roots and shoots that emerge from reactivated buds. During the first year, the growing shoots mature to woody stems. In the winter, these stems are cut back, and in the following spring, the cut stumps develop multiple shoots. The short-rotation coppice plantations are characterized by a very short, 2- to 3-year rotation, and the most productive varieties can produce up to 15 tons of oven-dried wood per hectare per year (Cunniff and Cerasuolo, 2011). The high-density willow plantations can also be efficiently used for heavy metal or organic phytoremediation, as reviewed by Marmiroli et al. (2011).

The biomass productivity of shrub willows is largely dependent on coppicing capability, early vigorous growth, shoot growth rate and final stem height, root system size, photosynthetic efficiency, formation and composition of woody stems, water and nutrient use, as well as abiotic and biotic stress tolerance. Genetic improvement of all these traits can be based on broad natural genetic resources represented by more than 400 species in the genus *Salix*. More than 200 species have hybrid origins, and ploidy levels vary from diploid up to

[1] This work was supported by the European Plant Phenotyping Network (grant no. 284443) and by grant no. GOP–1.1.1–11–2012–0365 from the Hungarian government.

* Address correspondence to dudits.denes@brc.mta.hu.

The author responsible for distribution of materials integral to the findings presented in this article in accordance with the policy described in the Instructions for Authors (www.plantphysiol.org) is: Dénes Dudits (dudits.denes@brc.mta.hu).

D.D. conceived the project and wrote and revised the article with contributions from all the authors; K.T. performed production and multiplication of genotypes; A.C. performed phenotyping; K.P. and I.V. performed photosynthetic measurements; A.V.N. and B.N. performed colchicine treatments and chromosome counting; L.S. performed informatics and data analyses; G.F. performed tetrapolyploidization; R.V. and P.D. performed hormone analysis; F.A. performed microscopy, statistical analyses, and coordination of experiments.

www.plantphysiol.org/cgi/doi/10.1104/pp.15.01679

dodecaploid (Suda and Argus, 1968; Newsholme, 1992). In addition to molecular marker-assisted clone selection, intraspecific and interspecific crosses have been shown to further extend genetic variability in breeding programs for biomass yield (Karp et al., 2011).

During natural diversification and artificial crossings of *Salix* spp., the willow genomes frequently undergo polyploidization, resulting in triploid or tetraploid allopolyploids. In triploid hybrids, both heterosis and ploidy can contribute to the improved biomass yield (Serapiglia et al., 2014). While the alloploid triploids have attracted considerable attention in willow improvement, the potentials of autotetraploid willow genotypes have not been exploited so far. As shown for other short-rotation wood species (poplar [*Populus* spp.], black locust [*Robinia pseudoacacia*], *Paulownia* spp., and birch [*Betula* spp.]), doubling the chromosome set by colchicine treatment can cause significant changes in organ morphology or growth parameters (Tang et al., 2010; Cai and Kang, 2011; Harbard et al., 2012; Mu et al., 2012; Wang et al., 2013a, 2013b). In several polyploidization protocols, the in vitro cultured tissues are exposed to different doses of colchicine or other inhibitors of mitotic microtubule function, and plantlets are differentiated from polyploid somatic cells (Tang et al., 2010; Cai and Kang, 2011). Alternatively, seeds or apical meristems of germinating seedlings can be treated with a colchicine solution (Harbard et al., 2012). Allotetraploids of poplar were produced by zygotic chromosome doubling that was induced by colchicine and high-temperature treatment (Wang et al., 2013a).

Since tetraploid willow plants with $2n = 4x = 76$ chromosomes are expected to represent novel genetic variability, especially for organ development and physiological parameters, a polyploidization project was initiated that was based on a highly productive diploid energy willow (*S. viminalis* var. Energo). Colchicine treatment of reactivated axillary buds of the in vitro-grown energy willow plantlets resulted in autotetraploid shoots and, subsequently, plants. For comparison of diploid and tetraploid variants of willow plants, digital imaging of green organs and roots was used for phenotyping. Among the tetraploid lines, genotypes were identified with improved biomass production, better photosynthetic parameters, and altered organ structure and hormone composition. The new tetraploid willow variants produced can serve as a unique experimental material to uncover key factors in biomass production in this short-rotation energy plant. In the future, these plants can also serve as crossing partners of diploid lines for the production of novel triploid energy willow genotypes.

RESULTS

Production of Autotetraploid Willow Plants by Colchicine Treatment of Axillary Buds in Vitro

Autotetraploid genotypes were produced by colchicine treatment of axillary bud meristems of willow plantlets cultured in Murashige and Skoog agar medium (see "Materials and Methods"). Several plantlets could be recovered after the treatment. These plantlets were grown and propagated in agar cultures. For early screening of DNA ploidy level, nuclei were isolated from root tips of stem cuttings for flow cytometric determination (Fig. 1). As shown by the histograms of flow cytometric analysis, plants of polyploid Energo (PP-E) lines have doubled DNA content in their root cells. These results were confirmed by chromosome counting using fluorescence microscopy (Fig. 1). Diploid Energo plants have a karyotype with $2n = 2x = 38$ chromosomes. Sixteen lines with $2n = 4x = 76$ chromosomes were identified by these tests. Plants with mixoploid root tissues were discarded. Both tetraploid and control diploid plantlets were transferred into soil and grown in the greenhouse. These plants were propagated by stem cuttings after rooting in water. At this step, the ploidy level was also checked by flow cytometry using nuclei isolated from roots. The screening and selection of lines with stable tetraploid nature were continued during propagation. Stem cuttings were also planted in the field, which allowed analyses of shoot regrowth under native environmental conditions. Independent tetraploid plantlets identified in in vitro cultures served as starting material for the establishment of tetraploid lines transferred to the soil in the greenhouse. In a subsequent comparison of diploid and tetraploid plants, several lines were used according to the availability of proper plant material.

Phenotyping Green Shoot Surface Area during Early Growth of Diploid and Tetraploid Energy Willow Plants

Based on studies with various plant species (Tackenberg, 2007; Golzarian et al., 2011; Fehér-Juhász et al., 2014), green pixel values reflecting leaf/shoot surface area are assumed to be directly proportional to the green mass of plants and can be used for the comparison of different genotypes. Dormant stem cuttings were planted in soil-containing special pots used in a phenotyping platform operating under controlled greenhouse conditions. Shoot development was monitored by digital photography, providing the green pixel-based average shoot surface area. As shown in Figure 2A, the analyzed tetraploid lines exhibited moderate differences in growth characteristics. Average values of shoot surface areas for PP-E2 and PP-E10 plants were higher than those for diploid plants at each sampling point during the 7-week experiment. PP-E13 plants, however, displayed lower average values for shoot surface area when compared with diploid plants. These statistically nonsignificant differences in green pixel number of shoots may arise from several factors such as shoot length, stem diameter, leaf number, leaf size, and petiole shape. Therefore, a detailed comparison of these organs from diploid and tetraploid plants was carried out under greenhouse and field conditions.

At the end of the 7-week phenotyping study, shoot length measurement showed 20% to 25% reduction in

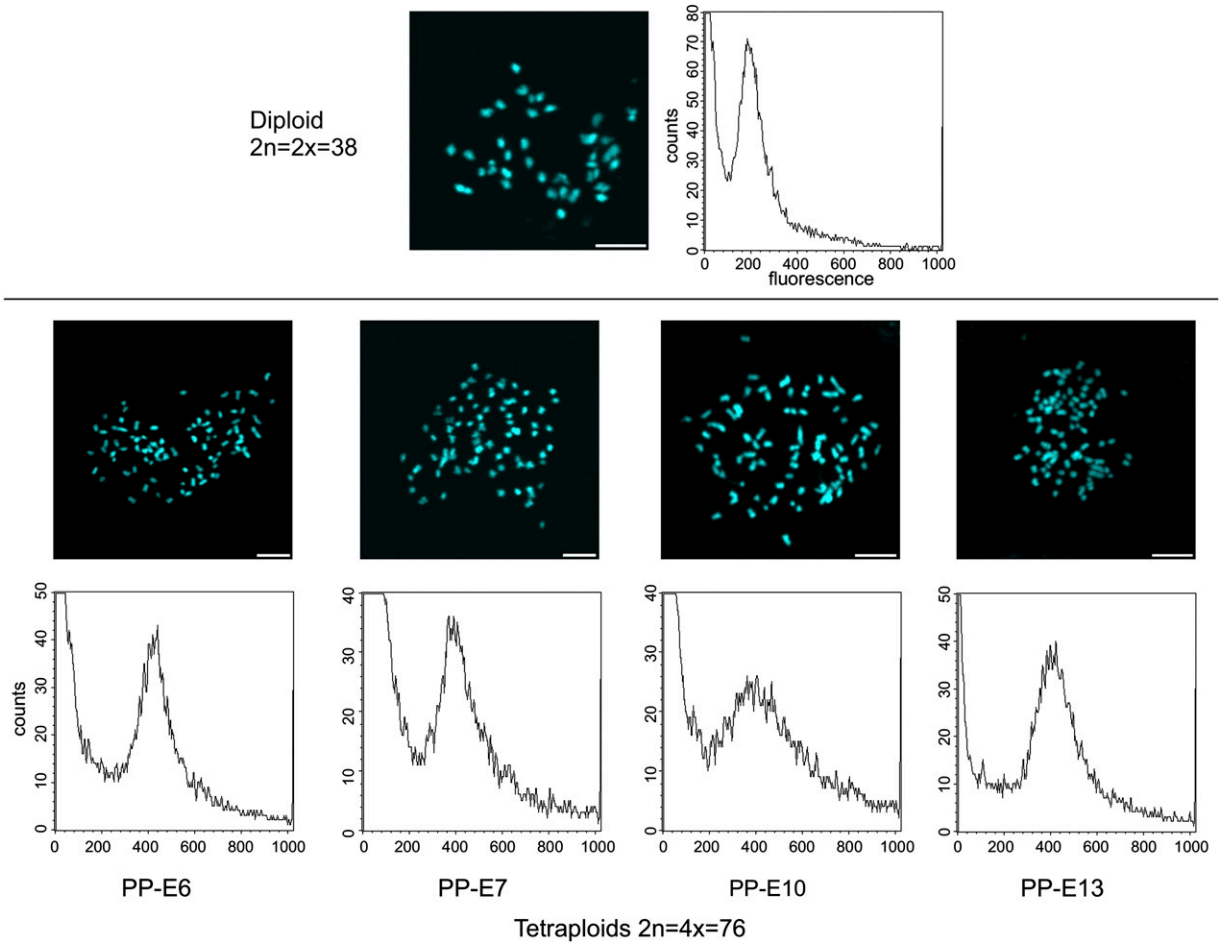

Figure 1. Identification of autotetraploid willow genotypes by chromosome counting (using 4′,6-diamidino-2-phenylindole [DAPI] stain) and flow cytometric analysis of relative DNA content (using propidium iodide). Shoots and plantlets that emerged from colchicine-treated axillary buds were rooted and sampled as described in "Materials and Methods." Representative data of at least three repetitions are shown. Bars = 5 μm.

primary shoot length of tetraploid plants relative to diploid plants (Figs. 2B and 3). This shortening of shoot length was linked to the enhanced secondary growth of shoots, which resulted in significantly wider stem diameters in several tetraploid genotypes, such as PP-E2, PP-E7, and PP-E13 (Fig. 2C; based on Welch's t test). Box-plot analysis revealed considerable variation in these parameters between individuals of the same autotetraploid genotype.

Growth characteristics observed in the greenhouse were also scored by monitoring shoot growth under field conditions in spring during the regrowth of shoots from dormant buds. As shown in Table I, the primary growth of all the tested tetraploid variants was reduced in comparison with the diploid plants. As a general trend, autotetraploidy slowed primary growth during the early shoot development of willow plants. To assess secondary growth characteristics, shoot diameters of the same plants were also measured (Table I). Without exception, plants of the tetraploid lines developed thicker stems on average. Selected genotypes (PP-E3, PP-E12, and PP-E13) showed statistically significant increases in secondary growth. The enlarged stem diameter of willow plants from several tetraploid genotypes (Figs. 2C and 4; Table I) can be related to substantial anatomical alterations as a consequence of doubled genome size. Cross sections of stems from older stem regions of willow plants revealed that wood formation between the primary and secondary xylem rings was increased significantly in the tested tetraploid plants relative to diploid plants. The bark region was also thicker in stems of the tetraploid plants than in diploid control plants (Fig. 4).

The Doubled Chromosome Set Alters the Shape, Size, Ultrastructure, and Hormone Composition of Willow Leaves

The phenotyping experiment demonstrated that the autotetraploid willow plants developed larger foliage (Fig. 3). Enlargement of leaves can originate from a set of characteristic changes at the cellular level. The

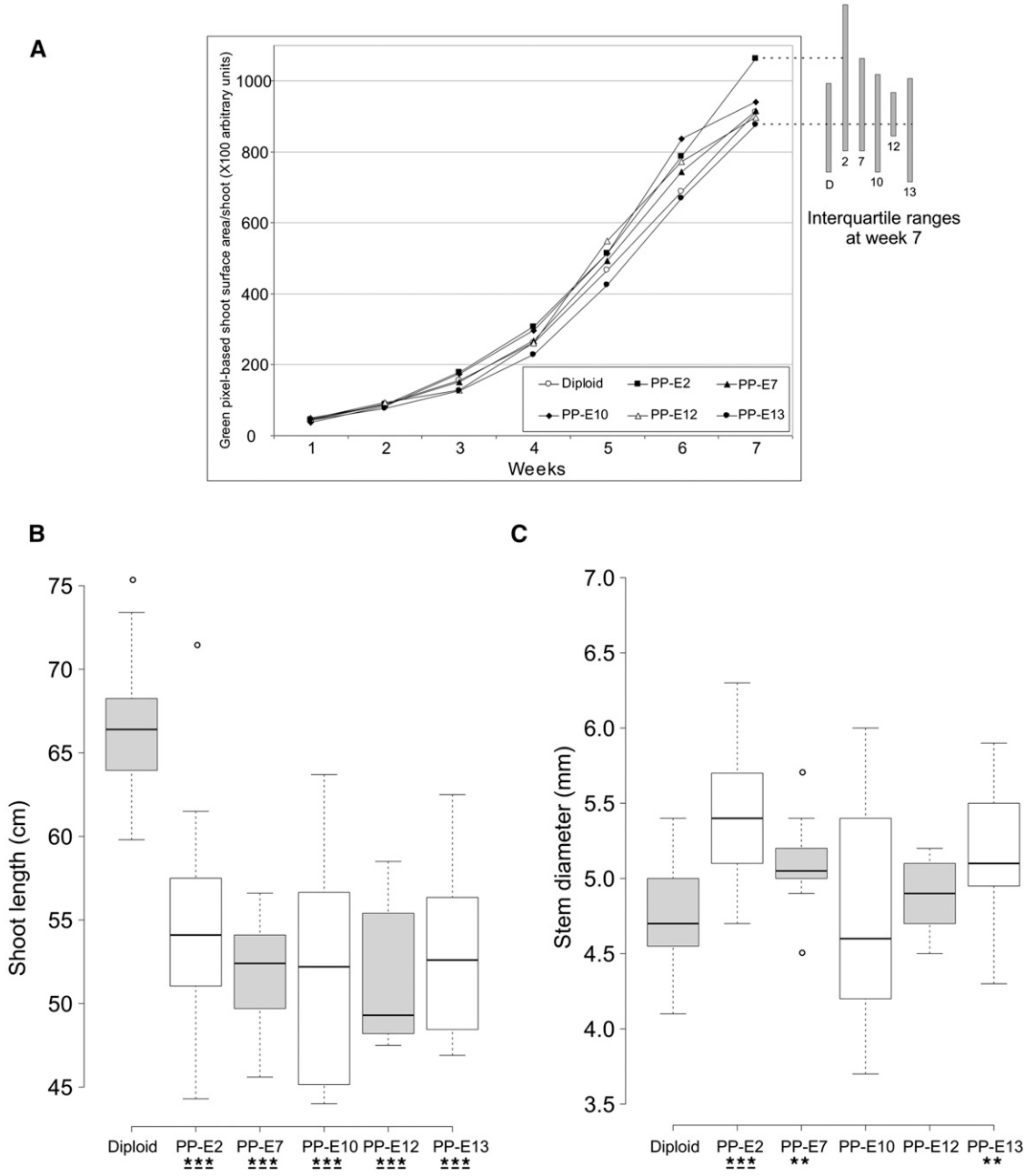

Figure 2. Variation in characteristics of shoot development in diploid and tetraploid genotypes of willow plants. A, Comparison of green pixel-based shoot surface area monitored by digital photography to record aboveground biomass growth of willow plants from different genotypes in the greenhouse. The graph extension at top right shows interquartile ranges (25th and 75th percentiles) at week 7 for corresponding data points. Seventh week data points having the lowest (PP-E13) and highest (PP-E2) mean values are connected to the corresponding interquartile ranges with dashed lines. B, Box-plot presentation of average shoot lengths after 7 weeks of growth shows reductions in primary growth of autotetraploid plants in comparison with diploid plants. C, Box-plot presentation of average stem diameter after 7 weeks of growth shows enhanced secondary growth of autotetraploid plants in comparison with diploid plants. Based on Welch's *t* test, statistically significant events compared with diploids are indicated below the sample labels as ***, $P < 0.01$ and **, $P < 0.05$. Underlined asterisks indicate the level of significance based on posthoc comparisons made with Tukey's honestly significant difference (HSD) test. Box-plot center lines show the medians; box limits indicate the 25th and 75th percentiles; whiskers extend 1.5 times the interquartile range from the 25th and 75th percentiles; outliers are represented by dots. Alternate boxes are shaded to differentiate neighboring boxes. n = 15, 15, 10, 11, 5, and 15 sample points.

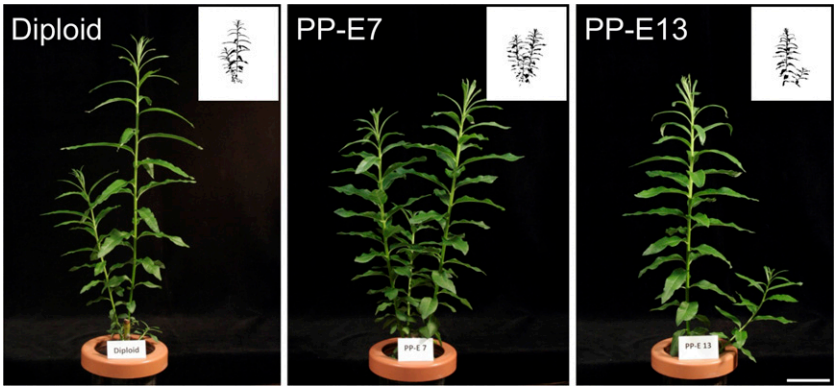

Figure 3. Altered plant architecture and growth characteristics of autotetraploid willow plants grown under greenhouse conditions. Stem cuttings were planted into cultivation pots, and the outgrowing shoots with characteristic phenotypic traits are presented. Note the development of larger, densely packed leaves of autotetraploid (PP-E7 and PP-E13) plants. Insets show thresholded binary images corresponding to the plants for a given view. Bar = 6.5 cm.

tetraploid plants produced significantly broader leaves than the diploid ones (Fig. 5, A and B). The width of leaf lamina was doubled in plants of tetraploid genotypes. Leaf lengths either increased or decreased moderately, varying among plants with various genotypes (Fig. 5, A and C). The cumulative effect of these size differences was reflected as a general trend of increased total leaf biomass for tetraploid plants (Fig. 5D).

Cross-section analysis of leaf midribs revealed an increase in the vein-xylem area in tetraploid leaves with enlarged leaf lamina (Fig. 6). Plants from all the studied tetraploid lines developed significantly thicker midribs. This anatomical feature was most prominent in PP-E7 plants, which displayed an average cross-sectional area of 0.72×10^6 μm^2. This value was twice as big as that of diploid samples (0.33×10^6 μm^2).

Beyond the described alterations in leaf morphology, major modifications at the cellular level were also detected by cytological analyses of leaf cross sections. The tetraploid palisade parenchyma cells were 50% larger than the diploids, as quantified by the cross-sectional area measurements (Fig. 7B). Due to this increase in cell size, fewer tetraploid cells were found per unit of distance (100 μm) along the parenchyma layer (Fig. 7C).

Several significant differences compared with diploid leaves were recognized in the cellular and organ structure of leaves of the tetraploid willow plants. These changes may have originated from an altered hormonal status of these leaves. Concentrations of the major plant hormones were compared in young expanded leaves of control diploid and selected tetraploid lines (Table II). The youngest fully developed leaves were compared in order to avoid the potential effect of different rates of leaf development among individual lines. The levels of active cytokinins (the sum of trans-zeatin, isopentenyladenine, cis-zeatin, and dihydrozeatin and the corresponding ribosides) differed among individual tetraploid lines, being either higher or lower than the corresponding values for control diploid samples. However, the concentration of the most physiologically active cytokinin, trans-zeatin, was enhanced in all tetraploid lines, and this increase was statistically significant in the case of line PP-E6. Substantially increased levels of cytokinin *N*-glucosides in all tested tetraploid plants indicate enhanced deactivation of active cytokinins and, thus, their higher turnover in tetraploids. The most dramatic increase was detected in GAs, namely the active GAs GA_4 and GA_7 (expressed as pmol g^{-1} fresh weight).

Table I. *Autotetraploidization generates opposite trends in alterations of the primary and secondary growth of shoots emerged from dormant buds in the field*

The reduced shoot length at both recording times reflects a slower primary growth rate in the early development of willow plants from the tetraploid variants. These plants developed wider stems, and the growth rate of stem diameter was increased as a consequence of genome duplication. The number of measured shoots ranged from 25 to 50 per genotype. Based on Welch's *t* test, statistically significant events compared with diploids are indicated as ***, $P < 0.01$, **, $P < 0.05$, and *, $P < 0.1$. Underlined asterisks indicate the level of significance based on posthoc comparisons made with Tukey's HSD test. The underlined dot indicates that the *P* value obtained by Tukey's test falls into the next higher rank of significance as compared with the significance level obtained by Welch's *t* test.

Genotypes	Shoot Height, Day 0	Shoot Height, Day 8	Primary Growth	Stem Diameter, Day 0	Stem Diameter, Day 8	Secondary Growth in Diameter
	cm		*cm 8 d^{-1}*	*mm*		*cm 8 d^{-1}*
Diploid	52.02 ± 3.79	83.08 ± 7.04	31.07 ± 4.24	5.76 ± 0.77	6.59 ± 0.60	0.82 ± 0.21
PP-E2	42.68 ± 2.39***	68.36 ± 4.57***	25.68 ± 0.99***	6.31 ± 0.41*	7.27 ± 0.71**	0.96 ± 0.35
PP-E3	39.48 ± 3.64***	64.96 ± 5.61***	25.48 ± 1.47***	6.33 ± 0.66	7.59 ± 0.68*·	1.26 ± 0.18***
PP-E4	38.60 ± 2.63***	63.90 ± 7.59***	25.30 ± 1.56**	6.33 ± 0.60*	7.22 ± 0.45*	0.89 ± 0.01
PP-E5	38.66 ± 2.20***	60.93 ± 4.28***	22.27 ± 2.69***	5.99 ± 0.54	7.01 ± 0.55	1.02 ± 0.22
PP-E6	36.46 ± 2.73***	58.74 ± 4.92***	22.28 ± 2.86***	5.87 ± 0.51	6.85 ± 0.63	0.98 ± 0.35
PP-E7	37.56 ± 2.55***	58.16 ± 3.24***	20.60 ± 4.99***	6.09 ± 0.50	6.76 ± 0.54	0.68 ± 0.17
PP-E12	42.09 ± 3.59**	69.76 ± 4.36**	27.67 ± 2.39**	5.90 ± 0.53	7.46 ± 0.64**	1.56 ± 0.21***
PP-E13	40.36 ± 2.74***	66.28 ± 4.41***	25.92 ± 2.28***	5.97 ± 0.50	7.12 ± 0.54*	1.15 ± 0.26***

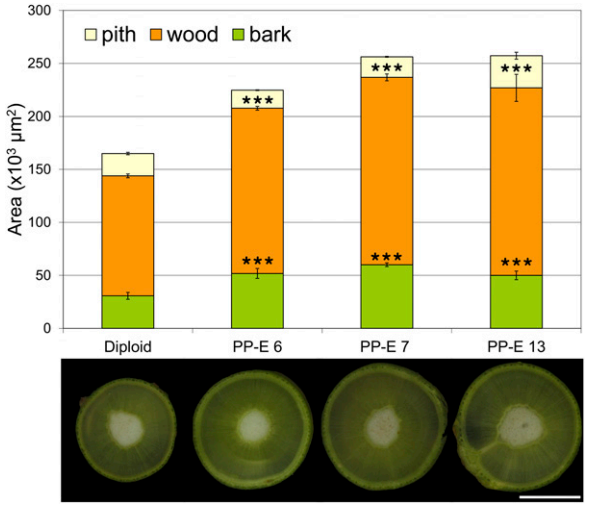

Figure 4. Wider stems with enlarged wood regions in stem sections of tetraploid willow plants. The chart shows the quantification of section areas representing bark, wood, and pith regions ($n = 4$). Statistically significant events (based on both Welch's t test and Tukey's HSD posthoc test) compared with diploids are indicated for wood and bark regions as ***, $P < 0.01$. Dissection microscope images of a set of cross sections are shown below the chart. Samples were collected at 120 cm from the shoot tip of plants. Bar = 0.5 cm.

The tetraploid leaves contained 4.1 to 5.89 times higher levels of GA_4. Two out of three tetraploid lines (PP-E7 and PP-E13) had GA_7 contents elevated by 57% to 75%. The concentrations of two stress hormones, salicylic acid and jasmonic acid, were almost doubled in the leaves of some autotetraploid genotypes compared with diploids. Differences in abscisic acid and indole-3-acetic acid contents were much less pronounced between diploid and tetraploid lines.

In relation to the above-described fundamental differences in leaf anatomy and shape between diploid and tetraploid genotypes, alterations in water metabolism may also be impacted after genome duplication. Tetraploid willow leaves were characterized by elevated stomatal conductance values (Fig. 8). Increased water utilization was characteristic for the majority of tetraploid plants. The stomata size of the tetraploid plants showed considerable variation. Enlarged stomata could be identified in certain genotypes (PP-E6, 27.55 ± 2.33 μm; and PP-E7, 23.24 ± 1.84 μm) in comparison with the diploid plants (21.31 ± 2.10 μm).

The Autotetraploid Energy Willow Genotypes Show Improved Net Photosynthetic CO_2 Uptake and Increased Electron Transfer Rate of PSI and PSII

The efficiency of atmospheric CO_2 uptake by plants and of its photosynthetic assimilation into organic compounds as the building blocks of biomass has a major impact on wood production capacity. In accordance with the stomatal conductance data, all tetraploid plants analyzed showed significantly enhanced CO_2 assimilation rate as compared with diploid plants (Fig. 9). Net photosynthetic CO_2 uptake rates per unit of leaf area have a positive linear relationship with the quantum yield of PSII or electron transfer rate (ETR), as shown by Kubota and Yoshimura (2002). Since the ETR is an estimate of the number of electrons passing through PSI and PSII, these associated parameters could be used for the prediction of photosynthetic capacity in leaves of different willow genotypes. Light saturation curves show increased rates of ETR(I) in tetraploid genotypes PP-E13 and PP-E6 under field conditions at higher light intensities (Fig. 10A). For PP-E13, ETR(II) was significantly greater, especially at PPFD values of 450 μmol photons m^{-2} s^{-1} or above (Fig. 10B). ETR(I) and ETR(II) values were generally lower in leaves of greenhouse-grown plants. Under these circumstances, the photosynthetic capacities of tetraploid variants were found to be improved, as indicated by both ETR(I) and ETR(II) values (Fig. 10, C and D).

In further characterization of the photosynthetic functions of willow plants with different genome sizes, a set of chlorophyll fluorescence parameters were analyzed to provide quantitative information about the physiological functionality of these plants (Baker, 2008). The OJIP chlorophyll fluorescence transient reflects electron transport through redox components of PSII and PSI (Strasser et al., 2004). As indicated by the spider plot in Figure 11, the tested genotypes showed clear differences in two fluorescence parameters. (1) PI describes the energy conservation between photons absorbed by PSII and the reduction of intersystem electron acceptors as well as the reduction of PSI end acceptors. Based on PI values, PP-E7, PP-E12, and PP-E13 plants exhibited the highest leaf photosynthetic activities. (2) Values of RC/ABS were higher in leaves of some tetraploid lines (PP-E7, PP-E13, and PP-E6).

Leaf chlorophyll content is the key parameter for characterization of the physiological performance of plants, including the determination of vegetation indices with woody species (Lu et al., 2015). Under greenhouse conditions, leaves of the tetraploid plants contained significantly greater concentrations of chlorophylls and carotenoids than the diploid plants (Table III). Elevated concentrations of these pigments were also detectable in field-grown leaves of the tetraploid variants relative to the diploid ones, but these differences did not reach statistically significant levels.

Enlarged Root System with Alterations in Anatomy and Hormonal Status as a Consequence of Autotetraploidization

Using the root phenotyping platform (Fig. 12A), growth of the root system was monitored by digital imaging from both side and bottom views. As shown in Figure 12A, the tetraploid PP-E12 plant developed an enlarged root system in comparison with the diploid plant. The differences are shown by images from both side and bottom views. Despite the fact that the

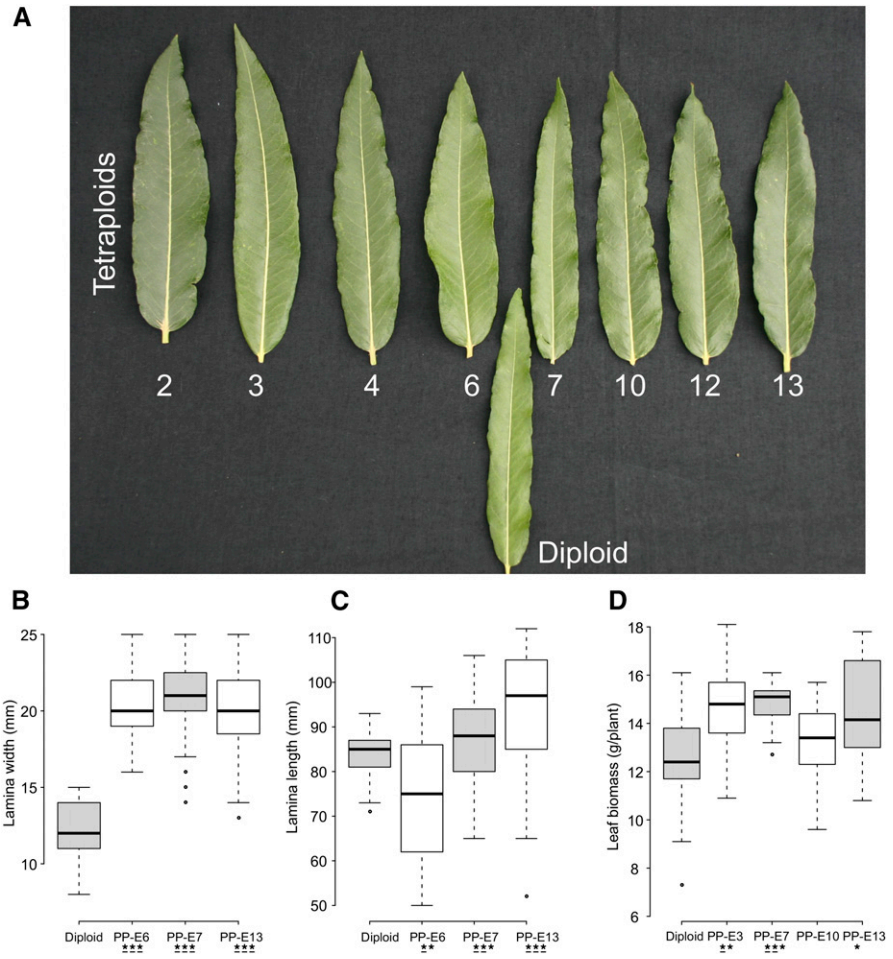

Figure 5. The autotetraploid genomic constitution of energy willow increases the foliage capacity of plants. A, Leaf morphology variations of willow plants grown in the field. B, Differences in leaf width between diploid and tetraploid willow plants grown in the greenhouse ($n > 52$). C, Differences in lamina length between diploid and tetraploid willow plants grown in the greenhouse ($n > 37$). D, Tetraploid willow plants produce more leaf biomass in comparison with diploid ones under greenhouse conditions ($n > 10$). Based on Welch's t tests, statistically significant events compared with diploids are indicated below the sample labels as ***, $P < 0.01$, **, $P < 0.05$, and *, $P < 0.1$. Underlined asterisks indicate the level of significance based on posthoc comparisons made with Tukey's HSD test. Box-plot center lines show the medians; box limits indicate the 25th and 75th percentiles; whiskers extend 1.5 times the interquartile range from the 25th and 75th percentiles; outliers are represented by dots.

cumulative white pixel counts generated cannot represent the whole-root biomass, this approach could be used for the detection of genotypic differences in root growth rate. During the first 3 weeks of root development, stem cuttings from tetraploid genotypes analyzed produced significantly higher root densities than cuttings from the diploid variant (Fig. 12B; based on Welch's t test). As the cultivation period proceeded, differences in root formation between tetraploid and diploid plants were increased considerably. In accordance with the data presented in Figure 12, the wet root weight data indicated that the autotetraploid willow plants produced a larger root system than the diploid plants after 7 weeks of growth (Fig. 13A). On the other hand, dry weight measurements showed that the differences between the genotypes were less pronounced, which may be due to different water contents (Fig. 13B).

Analysis of cross sections also revealed significant differences in anatomy between diploid and tetraploid roots. Root cortex cells were found to be larger in plants with duplicated genome size (Fig. 14).

Together with the observed morphological and cellular differences, changes in hormonal pools were also detected between diploid and tetraploid roots. The root tips and the elongation zones were sampled separately for hormone analyses. Since characteristic differences were detected predominantly in root tip samples, hormone concentrations in this tissue (expressed as pmol g^{-1} fresh weight) are presented in Table IV. All tetraploid lines showed elevated contents of active cytokinins, with the most significant changes found in the root tips of PP-E7 and PP-E13 plants. These lines also exhibited high levels of cytokinin phosphates (i.e. cytokinin precursors). In the PP-E plants, trans-zeatin contents significantly exceeded the value of diploid plants. Cytokinin storage forms (cytokinin *O*-glucosides) were elevated significantly in PP-E7 and PP-E13 roots. Root tips from two tetraploid lines (PP-E7 and PP-E13) contained extremely high amounts of indole-3-acetic acid. Elevated concentrations of salicylic acid were characteristic for all three tetraploid variants. Only in PP-E7 plants were GA_4 and GA_7 levels enhanced.

DISCUSSION

Identification of Energy Willow Variants with Duplicated Genome Size

Speciation in the genus *Salix* has taken place in nature by intraspecific or interspecific hybridizations that frequently resulted in allopolyploid progeny (Dorn, 1976, Barcaccia et al., 2003). Breeding for improved biomass

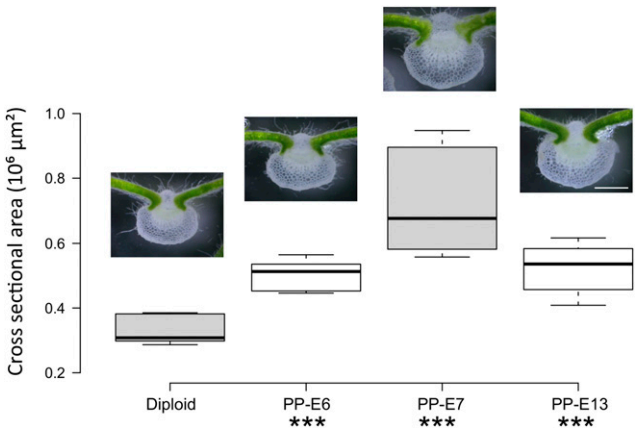

Figure 6. Enhanced midrib-xylem development in leaves from tetraploid plants compared with a diploid plant. Midrib cross-sectional areas were measured by manually tracing white-colored midrib regions sampled from the midpoint of each leaf. Representative images of hand-sectioned material are shown. Box-plot center lines show the medians; box limits indicate the 25th and 75th percentiles; whiskers extend 1.5 times the interquartile range from the 25th and 75th percentiles ($n = 9$). Statistically significant events (based on both Welch's *t* test and Tukey's HSD posthoc test) compared with diploids are indicated below the sample labels as ***, $P < 0.01$. Bar = 0.5 mm for all images.

yield of the shrub willow is preferentially based on crossing programs also generating allopolyploid genotypes (Serapiglia et al., 2014). This work provides a detailed characterization of autotetraploids to extend our knowledge about the morphological and developmental consequences of artificial genome duplication in this short-rotation energy willow. Autotetraploid woody crops have been produced in several species, including *Populus tremula* and *Populus pseudo-simonii* (Ewald et al., 2009; Cai and Kang, 2011), *Paulownia tomentosa* (Tang et al., 2010), *Acacia dealbata* and *Acacia mangium* (Blakesley et al., 2002), *R. pseudoacacia* (Ewald et al., 2009; Harbard et al., 2012; Wang et al., 2013a, 2013b), and *Betula platyphylla* (Mu et al., 2012). Colchicine, a microtubule polymerization inhibitor, has been used in a variety of methodologies involving the treatment of seeds or apical meristems of germinated seedlings. In vitro-cultured tissues with morphogenic potential can serve as ideal explants for the production of polyploid cells and regenerants (Tang et al., 2010; Cai and Kang, 2011).

In the case of the willow variety Energo, our attempts to establish tissue cultures with shoot differentiation had failed; therefore, the polyploidization protocol was optimized for the activation of axillary buds and the treatment of these organs with colchicine. One or 2 d after the removal of apical shoot meristems of willow plantlets grown in vitro, mitotic cells could be detected in cytological sections. Therefore, this early developmental stage of axillary meristems was selected for treatment with the anaphase inhibitor. The outgrowing shoots could be cut off and further cultured for root formation. Plantlets from colchicine-treated buds showed a characteristic variation in leaf and root morphology already in in vitro cultures. The wider, round-shaped leaves and thicker roots could serve as early markers for polyploid nature ($2n = 4x = 76$) that was confirmed by both chromosome counting and flow cytometry (Fig. 1).

Exposure of multicellular organs such as axillary buds to colchicine is expected to produce mixoploid cell populations including unaffected diploid cells in addition to tetraploid ones. Therefore, the outgrowing shoots may consist of diploid, chimeric, or tetraploid tissues. This cellular heterogeneity necessitates continuous testing of the ploidy level of propagated plants both in vitro and in the field. These studies revealed that the majority of the lines were represented only by tetraploid plants, and tetraploid shoots grew out from cuttings of these genotypes. Two of the lines propagated through cuttings produced diploid and tetraploid clones. In these unstable lines, diploid and tetraploid stems were recognized even on the same plant. This finding indicates that the observed variability of chromosome numbers can result from mixoploid nature or genome instability based on cellular events leading to different chromosomal compositions.

Autopolyploidy Can Alter Primary and Secondary Growth in Opposite Ways

Growth characteristics, including biomass accumulation, could be followed by color imaging of plants, which is one of the basic tools of plant phenotyping (Golzarian et al., 2011; Hartmann et al., 2011). Comparison of green surface area covered by green pixels, which can reflect shoot biomass, revealed essential differences between the diploid line and tetraploid lines (Fig. 2A). This phenotypic parameter indicates higher or lower green biomass productivities for tetraploid plants as compared with the diploid ones. The genetic background of the observed variation in traits of genotypes with the same chromosome numbers is not known. Independent genome duplication events can generate different genomic structures in the tetraploid lines. Variation in several phenotypic characters of independent autotetraploid birch families was also observed after colchicine treatment of seeds of this tree species (Mu et al., 2012).

The aboveground biomass of an individual shoot is an integrative parameter; therefore, analysis of individual morphological traits is needed to provide a deeper insight into the developmental consequences of genome size alteration. Shoot height and stem diameter data clearly showed contrasting changes in willow plants after duplication of their genome (Fig. 2, B and C; Table I). Reduction in stem length or growth rate was reported for various autotetraploid tree species (Särkilahti and Valanne, 1990; Griffin et al., 2015). Diploid *P. tomentosa* plants were found to be 10% taller than the tetraploids (Tang et al., 2010). Along with this trend, the mean height of the autotetraploid individuals of *B. platyphylla* was 19% lower than that of diploid birch plants (Mu et al., 2012). In our greenhouse study,

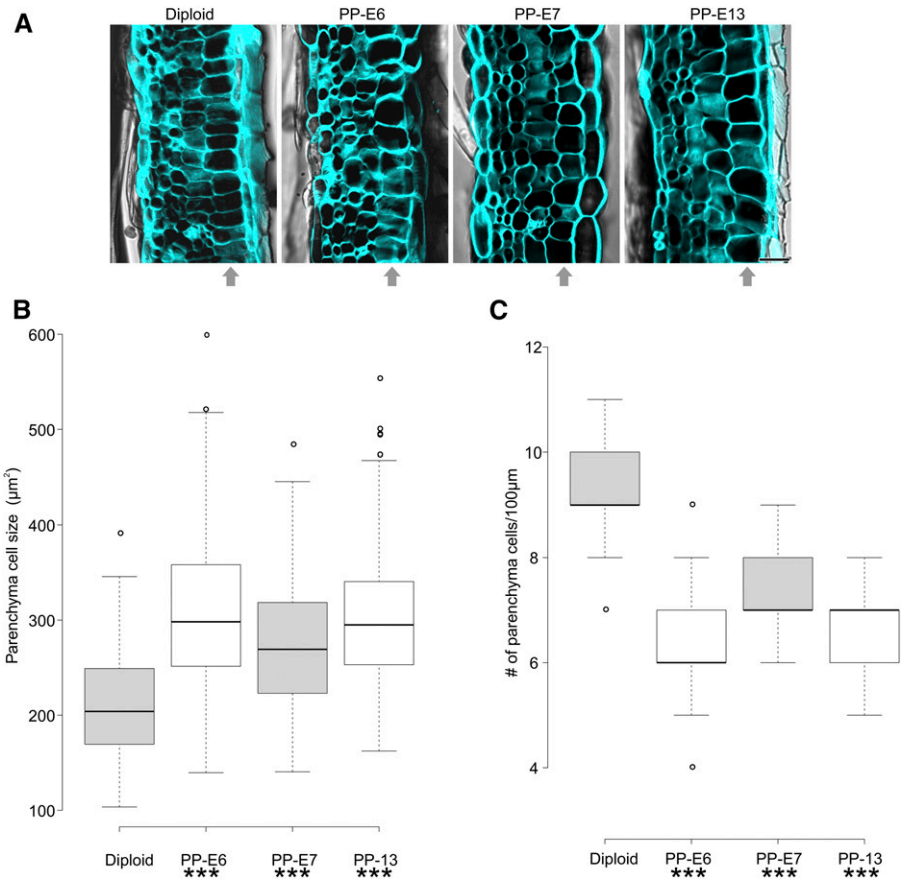

Figure 7. Tetraploid willow plants have enlarged palisade parenchyma cells. A, Comparison of leaf cross-sections from diploid and tetraploid willow plants. Calcofluor White-stained cell wall fluorescence (blue) was merged with transmission images. Arrows indicate the palisade parenchyma layer of leaves. Bar = 20 μm for all images. B, Quantification of average palisade parenchyma cell size as cross-sectional area (n = 200). C, Quantification of average number of parenchyma cells per 100-μm-long distance (n = 40). Box-plot center lines show the medians; box limits indicate the 25th and 75th percentiles; whiskers extend 1.5 times the interquartile range from the 25th and 75th percentiles; outliers are represented by dots. Statistically significant events (based on both Welch's t test and Tukey's HSD posthoc test) compared with diploids are indicated below the sample labels as ***, $P < 0.01$.

analysis of independent tetraploid lines indicated considerable variation in stem height, with the lines showing differences between the minimum and maximum values as well as the extent of the interquartile range (Fig. 2B). In agreement with other published examples (Tang et al., 2010; Mu et al., 2012), plants of several tetraploid willow lines (Fig. 2C; Table I) showed reduction in shoot height accompanied by wider stem formation as a consequence of autopolyploidization. The tetraploid *A. mangium* trees developed significantly thicker bark of stem compared with diploid trees (Harbard et al., 2012). Data presented in Figure 4 show that the most pronounced differences are found in the secondary xylem region, which resulted in enlarged wood sections of the analyzed tetraploid willow plants. Divergent changes caused by artificial genome doubling in primary and secondary aboveground growth of woody species are unexpected features, since these

Table II. *Autotetraploidization caused essential changes in the hormonal status of willow leaves*

The values presented show the amounts of different hormones as pmol g^{-1} fresh weight. Mature leaves from three plants were analyzed for each genotype. Based on Welch's t test, statistically significant events compared with diploids are indicated as ***, $P < 0.01$, **, $P < 0.05$, and *, $P < 0.1$. Underlined asterisks indicate the level of significance based on posthoc comparisons made with Tukey's HSD test. Underlined dots indicate that the P value obtained by Tukey's test falls into the next higher rank of significance as compared with the significance level obtained by Welch's t test.

Hormones	Diploid	PP-E6	PP-E7	PP-E13
Active cytokinins	5.91 ± 0.42	8.17 ± 1.01**	5.51 ± 2.09	5.47 ± 1.04
Trans-zeatin	0.67 ± 0.31	2.48 ± 1.48**	0.79 ± 0.13	0.72 ± 0.25
Cytokinin phosphates	1.64 ± 0.51	2.41 ± 0.57	0.92 ± 0.27	1.55 ± 1.02
Cytokinin *O*-glucoside	25.71 ± 2.40	25.67 ± 2.43	20.66 ± 3.57	18.27 ± 3.45**
Cytokinin *N*-glucosides	9.49 ± 0.26	13.76 ± 2.02*·	10.94 ± 0.68*	14.52 ± 1.54**·
Abscisic acid	96.29 ± 11.78	94.67 ± 6.71	93.78 ± 16.00	79.51 ± 4.61
Indole-3-acetic acid	47.06 ± 4.73	40.18 ± 4.57	49.46 ± 6.45	41.21 ± 3.27
Salicylic acid	1,288.85 ± 87.31	2,376.65 ± 214.78***	2,387.01 ± 437.79**	2,520.09 ± 586.93*·
Jasmonic acid	6.92 ± 0.51	9.16 ± 1.37*	14.10 ± 4.05*·	10.08 ± 2.56
Jasmonate-Ile	1.49 ± 0.19	1.76 ± 0.71	2.77 ± 0.39**	2.65 ± 0.29***
GA_4	0.78 ± 0.35	4.60 ± 1.22**·	3.20 ± 1.03**	3.23 ± 0.98**
GA_7	41.55 ± 18.25	32.36 ± 7.80	72.87 ± 18.67**	65.48 ± 19.97**

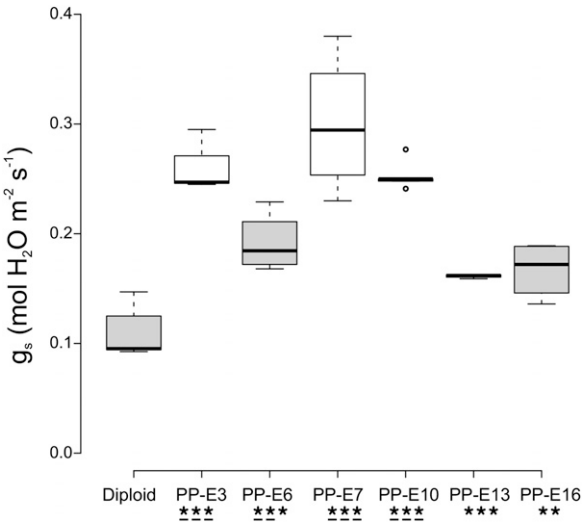

Figure 8. Tetraploid willow plants transpire more water, as shown by the elevated stomatal conductance in leaves. Leaf stomatal conductance (g_s) was measured on the fifth/sixth fully developed younger leaves (from top) of willow plants. The measurements were recorded in an air CO_2 concentration of 400 μg mL^{-1}, leaf temperature of 22°C, and photosynthetic active radiation of 400 to 430 μmol photons m^{-2} s^{-1} ($n = 5$). Box-plot center lines show the medians; box limits indicate the 25th and 75th percentiles; whiskers extend 1.5 times the interquartile range from the 25th and 75th percentiles; outliers are represented by dots. Based on Welch's *t* test, statistically significant events compared with diploids are indicated below the sample labels as ***, $P < 0.01$ and **, $P < 0.05$. Underlined asterisks indicate the level of significance based on posthoc comparisons made with Tukey's HSD test.

two functions correlate in nature, as shown by studies on Mediterranean subshrub species (Camarero et al., 2013). A similar synchrony between primary and secondary growth was also recorded over the growing season in boreal conifers (Huang et al., 2014). All these observations indicate the existence of a regulatory mechanism coordinating parameters of organ growth that differs between diploid and autotetraploid plants of these tree species.

Apical meristems play a central role in the control of shoot growth. At present, basic information revealing the molecular or cellular bases of the reduced primary growth of autotetraploid tree stems is still missing. Comparison of the transcript profiles of tender shoot tips from diploid and tetraploid birch trees indicated several thousand differentially expressed genes. Up-regulation of genes involved in the biosynthesis or signal transduction of auxin and ethylene was detected in tetraploid shoot meristems (Mu et al., 2012). Genes of APETALA2/ETHYLENE RESPONSIVE FACTOR (AP2/ERF) domain-containing and AP2 domain class transcription factors were significantly activated in tetraploid meristems relative to diploids (Mu et al., 2012). As reviewed by Licausi et al. (2013), ectopic expression of selected AP2/ERF protein genes can result in growth retardation with simultaneous up-regulation of defense- or stress-related genes. This hypothetic explanation of the reduced growth of tetraploids needs experimental confirmation, especially with consideration of the extremely large size and divergent roles of the AP2/ERF superfamily. Rao et al. (2015) predicted 173 AP2/ERF genes in the *Salix arbutifolia* genome.

The reduction of stem growth observed in the tetraploid willow plants is further supported by the 4.1- to 5.9-fold increase in active GA (GA_4 and GA_7) content in tetraploid leaves as compared with diploid plants (Table II). In transgenic poplar (*P. tremula* × *Populus alba*) plants, active GA levels were increased by ectopic expression of the GA-INSENSITIVE (GAI) or REPRESSOR OF GAI-LIKE genes, which caused variable degrees of semidwarfism in these trees (Elias et al., 2012). An increase in the levels of various endogenous GAs was correlated with the extent of growth reduction. For example, the abundance of the inactive precursor GA_{20} in transgenic lines was increased 2.5- to 5-fold, and the heights of field-grown transformants reached only 93% to 63% of the wild-type plants. In contrast to the willow tetraploids, the shoot diameters of these transgenic poplar trees were also reduced. In another experimental system, hybrid poplar clones (*P. tremula* × *P. alba*) were transformed for RNA interference down-regulation of C19 gibberellin 2-oxidase (GA2ox) genes (Gou et al., 2011). Suppression of *PtGA2ox4* and *PtGA2ox5* genes resulted in elevated GA_1 and GA_4 concentrations, with simultaneous increase in leaf biomass and elongation of xylem fiber length and width in aboveground stems. In an earlier study, the Arabidopsis complementary DNA

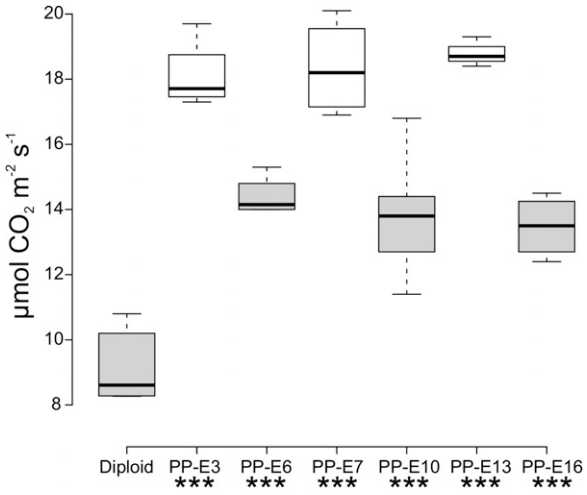

Figure 9. Autotetraploid willow plants absorb CO_2 more efficiently from the atmosphere. The rate of net CO_2 fixation was measured on the fifth/sixth fully developed young leaves (from top) of willow plants at 400 to 430 μmol photons m^{-2} s^{-1} light intensity, 22°C temperature, and 400 μg mL^{-1} ambient CO_2 level ($n = 5$). Box-plot center lines show the medians; box limits indicate the 25th and 75th percentiles; whiskers extend 1.5 times the interquartile range from the 25th and 75th percentiles. Statistically significant events (based on both Welch's *t* test and Tukey's HSD posthoc test) compared with diploids are indicated below the sample labels as ***, $P < 0.01$.

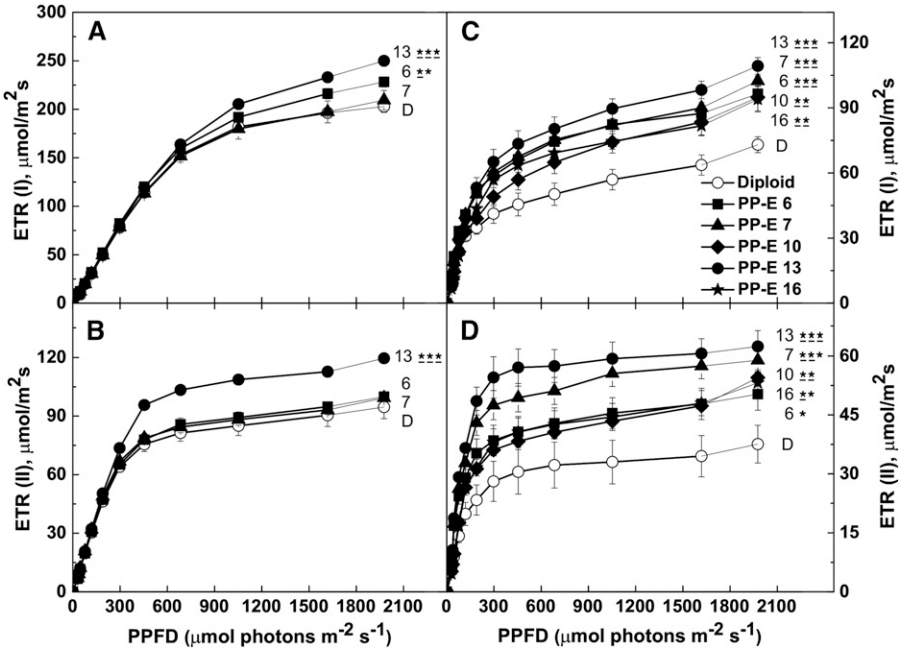

Figure 10. Improved photosynthetic capacity of tetraploid willow plants as indicated by ETRs of PSI and PSII measured on leaf samples. Simultaneous light response curves of ETR(I) and ETR(II) were measured in the dark-adapted fifth/sixth fully developed young leaves (from top) for both field and greenhouse genotypes using Dual PAM as described in "Materials and Methods." A, ETR (I) under field conditions. B, ETR(II) under field conditions. Leaves of field-grown plants were collected in wet tissue and kept in an ice box, and ETR measurements were carried out within 2 h of sample collection. C, ETR(I) under greenhouse conditions. D, ETR (II) under greenhouse conditions. Tetraploid willow genotypes are indicated as black symbols and the diploid genotype by white symbols. Data are means ± SE of six independent plants per genotype. Based on Welch's *t* test, statistically significant events (for the highest photosynthetic photon flux density [PPFD] measurement) compared with diploids are indicated next to corresponding data points as ***, $P < 0.01$, **, $P < 0.05$, and *, $P < 0.1$. Underlined asterisks indicate the level of significance based on posthoc comparisons made with Tukey's HSD test.

for GA 20-oxidase (*AtGA20ox1*) was overexpressed in hybrid aspen, *P. tremula* × *Populus tremuloides* (Eriksson et al., 2000). The transgenic plants produced high levels of 13-hydroxylated C19 GAs (GA_{20}, GA_1, and GA_8) and non-13-hydroxylated C19 GAs (GA_9, GA_4, and GA_{34}) in both internodes and leaves. Consequently, these transgenic trees showed enhanced growth. The cited results from transgenic modification of GA metabolism in poplar can help explain certain characteristics of our autotetraploid willow genotypes. Considering the complexity of hormonal status modification in PP-E plants, as shown in Table II, the potential involvement of additional factors, such as high concentrations of salicylic and jasmonic acids, cannot be excluded from regulators of primary growth of these plants with duplicated genomes. As reviewed by Rivas-San Vicente and Plasencia (2011), in addition to its functions in biotic and abiotic stress responses, salicylic acid plays a crucial role in growth and development regulation in coordination with other plant hormones. The cross talk between salicylic acid and GA can be relevant in the interpretation of the traits of polyploid willow plants. Alonso-Ramírez et al. (2009) showed that GAs were able to increase salicylic acid biosynthesis under stress conditions.

At present, only limited knowledge is available on the molecular or cellular mechanisms underlying the enhanced secondary growth of autotetraploid tree stems that was observed here and in other studies (Särkilahti and Valanne, 1990; Harbard et al., 2012; Mu et al., 2012; Griffin et al., 2015). In plants, three main types of meristematic tissues occur: shoot and root apical meristems and procambium in vascular tissues. During wood formation, vascular cambium activity and differentiation of secondary xylem from vascular cells are under a complex hormonal control (for review, see Ye and Zhong, 2015). The vascular cambium is regulated by the two major plant hormones, auxin and cytokinins (Růžička et al., 2015). High expression of cytokinin biosynthetic genes as well as high endogenous levels of cytokinins were found in xylem precursor cells (Ohashi-Ito et al., 2014). Cytokinins are considered central regulators of cambial activity (Matsumoto-Kitano et al., 2008). This role of cytokinin is in accordance with enhanced active cytokinin levels and stimulation of wood development in tetraploid willow lines. Apart from cytokinins and auxins, GAs, ethylene, and brassinosteroids are also involved in the control of xylem development (Didi et al., 2015). The pivotal role of GAs was shown by studies on transgenic poplar trees. RNA interference suppression of two members (*PtGA2ox4* and *PtGA2ox5*) of the C19 GA2ox gene subfamily significantly increased the number of cells in the cambium zone

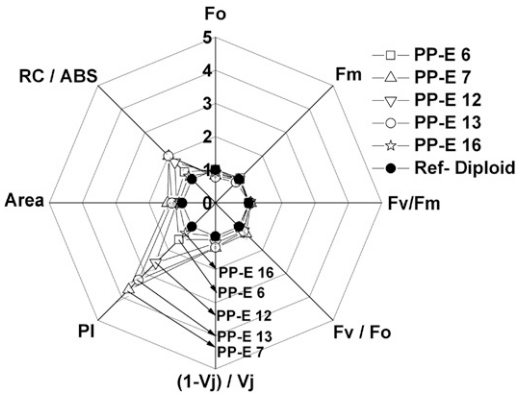

Figure 11. Spider plot of chlorophyll fluorescence parameters deduced from OJIP fast kinetics measurements. Shown are the values of initial (F_o) and maximal (F_m) fluorescence levels, the F_v/F_m and F_v/F_o (maximal PSII quantum yield) ratios, the $(1 - V_j)/V_j$ parameter, where $V_j = (F_{2ms} - F_o)/F_v$, the performance index (PI), the area parameter, as well as the dissipated energy flux per active reaction center (RC/ABS) measured on fifth/sixth young fully developed leaves. The data are shown for the tetraploid lines (white symbols) after normalization to respective values obtained in the diploid line (black symbols). Data are means ± SE of six to seven independent greenhouse-grown plants per genotype.

(Gou et al., 2011). In leaves of these transgenic poplar plants, both GA_1 and GA_4 levels were increased 1.4- and 1.9-fold, respectively, relative to control leaves. These transgenic plants developed wider stem diameters. The variety of transgenic approaches has been widely used for tree improvement (Dubouzet et al., 2013). Our production of tetraploid willow genotypes with extended secondary xylem tissues and wider stems, in combination with improved photosynthesis and enhanced root biomass, can provide an example for the generation of novel genetic variation to improve traits of short-rotation woody crops by nontransgenic means.

Duplication of the Willow Genome Directs Leaf Functions toward Improving Biomass Production

Comprehensive characterization of several independent autotetraploid lines of energy willow revealed substantial changes in leaf structure and functions as consequences of genome size modification. Increase of leaf biomass (Fig. 5D) is accompanied by alterations in leaf shape (Fig. 5A) and extended lamina length and width (Fig. 5, B and C). These characteristic phenotypic traits were also reported for other autotetraploid tree variants (Ewald et al., 2009; Cai and Kang, 2011; Harbard et al., 2012; Mu et al., 2012). Cellular events beyond the ploidy-driven enlargement of leaves are poorly understood in the case of tree species. Detailed analysis of diploid and autotetraploid cultivars of two grass species, *Lolium perenne* and *Lolium multiflorum*, showed that the bigger leaf size of polyploids resulted mainly from the increased cell elongation rate but not from the longer duration of the elongation period. The increased final cell size also contributed to organ size change (Sugiyama, 2005). A kinematic method showed no significant differences in cell division parameters, such as cell production rate and cell cycle duration, between the diploid and tetraploid cultivars. In tetraploid willow leaves, fewer but larger palisade parenchyma cells were detected (Fig. 7). These characteristics were also detected in autotetraploid *Pennisetum americanum* and *Medicago sativa* leaves, where increased cell size and fewer cells per unit of leaf area were detected (for review, see Warner and Edwards, 1993). Plant organ size is dependent on growth that is driven by cell division and expansion. Both of these processes are regulated by phytohormones (Nelissen et al., 2012). In the division zone of maize (*Zea mays*) leaves (i.e. in meristematic tissues), elevated concentrations of auxin (indole-3-acetic acid) and cytokinins (trans-zeatin and isopentenyladenine) were detected in comparison with mature or even senescing parts of leaves.

Exogenous cytokinin was reported to modulate the leaf shape (De Lojo and Di Benedetto, 2014). Peaks of GAs were found at the transition zone. Comparison of hormone contents of expanded diploid and tetraploid willow leaves provided characteristic indicators to explain size alterations. As shown by Table II, indole-3-acetic acid levels did not differ significantly between the analyzed genotypes. However, all tetraploid lines exhibited elevated levels of the most physiologically active cytokinins, including trans-zeatin. At the same time, enhanced cytokinin *N*-glucoside levels in tetraploids can be an indication of the promoted deactivation of active cytokinins and, thus, their higher turnover in tetraploid lines. The observed significant increase in GA_4 and GA_7 contents observed in tetraploid leaves can be considered as a potential factor in

Table III. *Leaf chlorophyll (Chl) and total carotenoid (Car) contents of diploid and tetraploid plants grown under field and greenhouse conditions*

Sampling was carried out from the fifth/sixth fully developed young leaves (from top). Data are means ± SE (μg cm^{-2}) of six to seven independent plants per genotype. Based on Welch's *t* test, statistically significant events compared with diploids are indicated as ***, $P < 0.01$. Underlined asterisks indicate the level of significance based on posthoc comparisons made with Tukey's HSD test.

Genotypes	Field-Grown Plants				Greenhouse-Grown Plants			
	Chl *a*	Chl *b*	Chl (*a* + *b*)	Car (*x* + *c*)	Chl *a*	Chl *b*	Chl (*a* + *b*)	Car (*x* + *c*)
Diploid	48.68 ± 1.4	17.47 ± 0.5	65.32 ± 1.9	12.15 ± 0.25	18.50 ± 0.48	5.3 ± 0.24	23.56 ± 0.58	3.84 ± 0.13
PP-E6	51.60 ± 1.3	18.49 ± 0.5	69.22 ± 1.7	12.38 ± 0.22	22.02 ± 0.58***	6.5 ± 0.19***	28.17 ± 0.75***	4.45 ± 0.12***
PP-E7	49.71 ± 1.5	18.50 ± 0.4	67.35 ± 1.8	12.07 ± 0.22	22.66 ± 0.94***	6.6 ± 0.32***	28.96 ± 1.25***	4.58 ± 0.16***
PP-E13	49.84 ± 2.2	18.17 ± 0.8	67.15 ± 3.0	11.74 ± 0.33	23.34 ± 0.71***	6.6 ± 0.25***	29.59 ± 0.91***	4.62 ± 0.12***

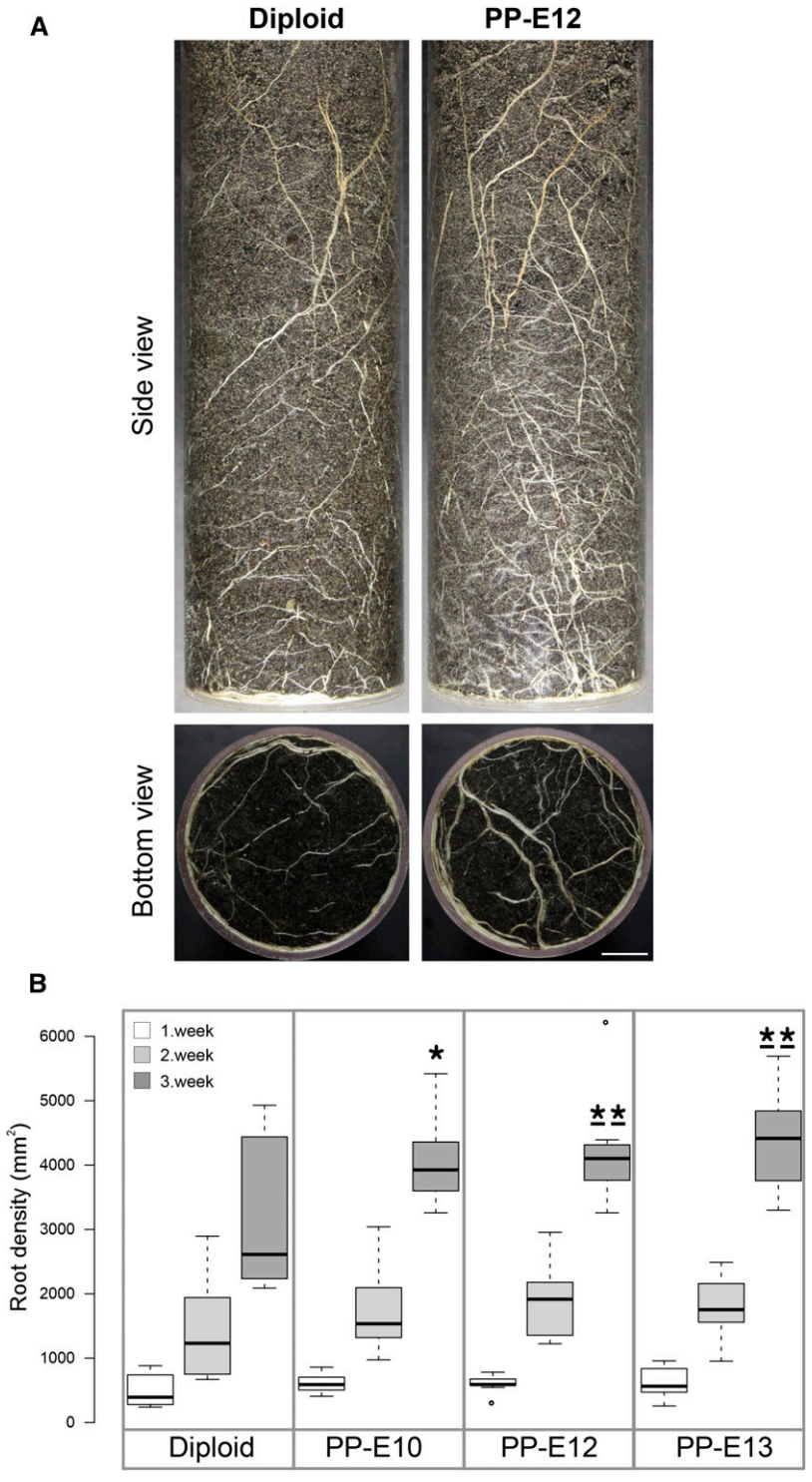

Figure 12. Significant stimulation of root development after duplication of the genome size of energy willow. A, Side and bottom views of roots from the diploid and tetraploid (PP-E12) plants grown in soil in transparent wall plexiglass columns. Digital images were taken at week 3 of cultivation. Bar = 2 cm for all images. B, Total surface area (in mm^2) occupied by white pixels was used to monitor root biomass growth to compare diploid and tetraploid willow plants during early development. Box-plot center lines show the medians; box limits indicate the 25th and 75th percentiles; whiskers extend 1.5 times the interquartile range from the 25th and 75th percentiles; outliers are represented by dots. Based on Welch's *t* test, statistically significant events compared with diploids are indicated as **, $P < 0.05$ and *, $P < 0.1$. Underlined asterisks indicate the level of significance based on posthoc comparisons made with Tukey's HSD test. $n = 10$ sample points.

causing the enlargement of tetraploid willow leaves. This hypothesis is supported by studies on maize leaf development (Nelissen et al., 2012). Both the leaf elongation rate and the size of the division zone were increased in transgenic maize plants with elevated GA levels through the overproduction of the AtGA20ox1 enzyme. The GA-based interpretation of ploidy-induced alterations in willow leaf morphology is supported by studies of transgenic hybrid aspen overexpressing the GA20ox gene (Eriksson et al., 2000). The increased level of GAs in fully expanded transgenic leaves caused the development of longer and broader leaves, resulting in higher leaf fresh weights.

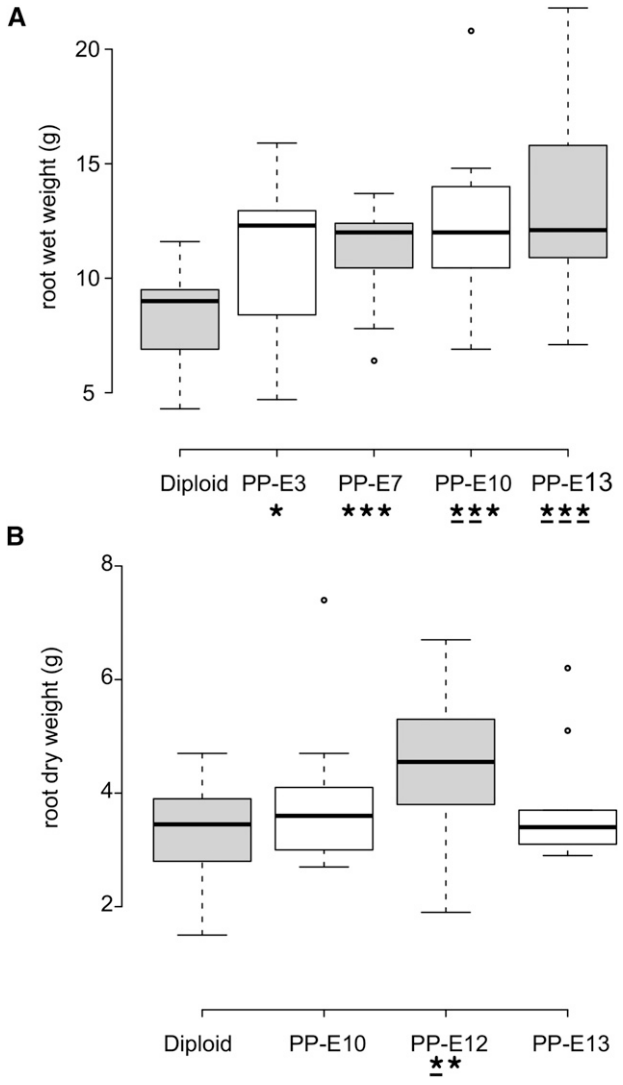

Figure 13. Autotetraploidization resulted in energy willow genotypes with increased root biomass. A, Experiment 1. Plants from tetraploid genotypes developed significantly more root than the control diploid ones based on fresh weight measurements (g plant^{-1}; $n = 10$). B, Experiment 2. Increased root biomass of tetraploid willow genotypes as compared with diploid plants based on dry weight measurements (g plant^{-1}; $n = 10$). Box-plot center lines show the medians; box limits indicate the 25th and 75th percentiles; whiskers extend 1.5 times the interquartile range from the 25th and 75th percentiles; outliers are represented by dots. Based on Welch's t test, statistically significant events compared with diploids are indicated below the sample labels as ***, $P < 0.01$, **, $P < 0.05$, and *, $P < 0.12$. Underlined asterisks indicate the level of significance based on posthoc comparisons made with Tukey's HSD test.

The experimental findings presented here indicate that the enlargement of foliage size generated by autotetraploidy was accompanied by improvement of the photosynthetic productivity of tetraploid willow plants. Increases in both the stomatal conductance and the CO_2 assimilation rate can be a prerequisite for the potential improvement of biomass yield (Figs. 8 and 9). Similarly, these parameters were reported to be superior for tetraploid black locust even under salt stress (Wang et al., 2013b). In earlier studies on the polyploids of *Atriplex confertifolia*, photosynthetic rates per cell were highly correlated with ploidy level and with the

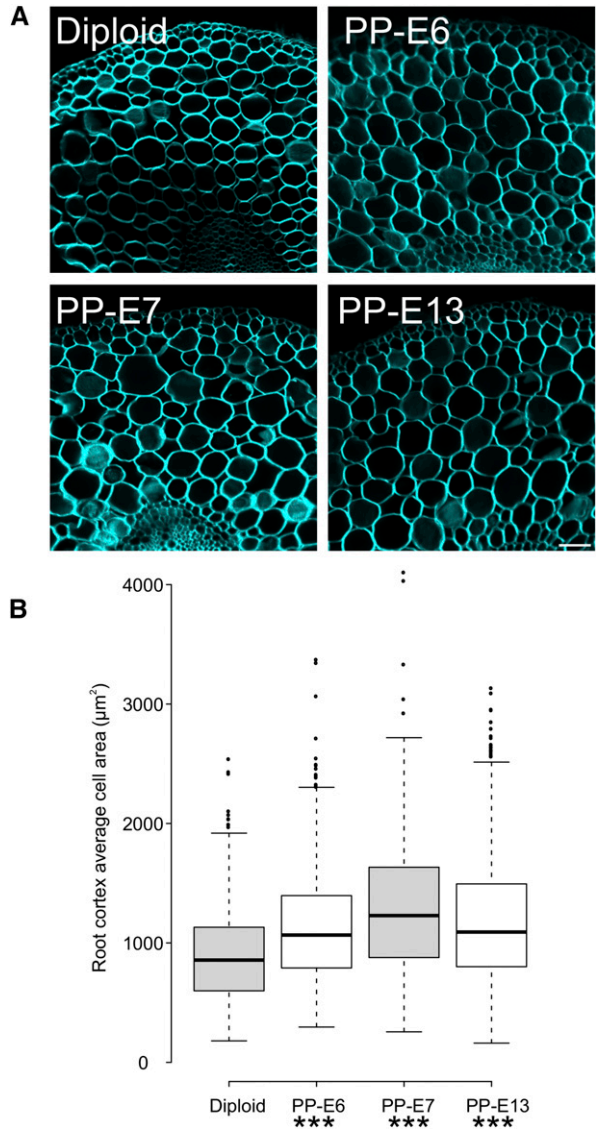

Figure 14. Differences in root anatomy detected between diploid and tetraploid willow plants. A, Calcofluor White-stained, hand-sectioned roots (from the maturation zone) of diploid and tetraploid plants were imaged using confocal laser scanning microscopy. Note the larger cortical cells of the tetraploid samples. Bar = 50 μm for all images. B, Cortical cells of diploid and tetraploid roots were manually traced on hand-sectioned material using Olympus Fluoview software, and average cross-sectional areas of cortical cells were calculated and plotted for diploid and tetraploid samples ($n > 362$). Box-plot center lines show the medians; box limits indicate the 25th and 75th percentiles; whiskers extend 1.5 times the interquartile range from the 25th and 75th percentiles; outliers are represented by dots. Statistically significant events (based on both Welch's t test and Tukey's HSD posthoc test) compared with diploids are indicated below the sample labels as ***, $P < 0.01$.

Table IV. *Root tips from tetraploid plants differed from those of diploid plants in hormone contents*

Stem cuttings were rooted in water for 2 weeks, and 5- to 8-mm root tips were collected for hormone analysis. The values presented show the amounts of different hormones as pmol g^{-1} fresh weight. Roots from three plants were analyzed for each genotype. Based on Welch's *t* test, statistically significant events compared with diploids are indicated as ***, $P < 0.01$, **, $P < 0.05$, and *, $P < 0.1$. Underlined asterisks indicate the level of significance based on posthoc comparisons made with Tukey's HSD test. Underlined dots indicate that the *P* value obtained by Tukey's test falls into the next higher rank of significance as compared with the significance level obtained by Welch's *t* test.

Hormones	Diploid	PP-E6	PP-E7	PP-E13
Active cytokinins	25.04 ± 2.25	27.88 ± 2.79	52.36 ± 6.12***	40.68 ± 3.96***
Trans-zeatin	1.37 ± 1.04	2.71 ± 0.92***	4.86 ± 1.59***	2.88 ± 0.32***
Cytokinin phosphates	17.92 ± 2.20	20.08 ± 2.13	33.97 ± 2.58***	11.19 ± 0.94**
Cytokinin *O*-glucoside	2.09 ± 0.72	2.18 ± 0.83	11.90 ± 0.78***	6.49 ± 0.60***
Cytokinin *N*-glucoside	0.38 ± 0.14	0.17 ± 0.09	0.42 ± 0.02	0.36 ± 0.09
Abscisic acid	55.61 ± 11.90	45.11 ± 4.81	49.41 ± 8.00	24.46 ± 4.04**.
Indole-3-acetic acid	234.16 ± 10.28	197.91 ± 21.35*	890.72 ± 96.54***	639.72 ± 55.75***
Salicylic acid	184.75 ± 23.28	308.82 ± 18.20***	322.27 ± 27.77***	241.44 ± 30.48*
Jasmonic acid	1,150.00 ± 189.18	1,119.63 ± 132.60	1,072.51 ± 101.23	834.16 ± 37.72*
Jasmonate-Ile	148.65 ± 48.20	120.19 ± 16.44	157.46 ± 20.39	118.99 ± 17.86
GA_4	1.06 ± 0.12	1.07 ± 0.44	1.42 ± 0.06**	0.51 ± 0.59
GA_7	0.46 ± 0.13	0.70 ± 0.64	2.02 ± 1.58*.	1.17 ± 0.59

activity of ribulose 1,5-bisphosphate carboxylase per bundle sheath cell (Warner and Edwards, 1989). In other autotetraploid species (*M. sativa* and *P. americanum*), doubled cell volume was accompanied by lower cell number per unit of leaf area; subsequently, the higher ploidy levels did not result in a change in the rate of photosynthesis per leaf area (for review, see Warner and Edwards, 1993). A similar conclusion was drawn from studies on a natural allotetraploid (*Glycine dolichocarpa*), where the light-saturated ETR per cell was higher in the tetraploids with reduced numbers of palisade cells (Coate et al., 2012).

In this study, the improvement of photochemical reactions was recorded by monitoring the ETR of PSI and PSII. Light response curves of PSI and PSII revealed higher rates per unit of leaf area in the tetraploid leaves analyzed from plants grown under both field and greenhouse conditions (Fig. 10). Differences between diploid and tetraploid genotypes in ETR values of PSII were, in general, larger in plants grown in the greenhouse. Higher ETR values were reported for the tetraploid Japanese honeysuckle (*Lonicera japonica*) cultivar than for the diploid one. Reduction of ETR by drought was smaller in this genotype (Li et al., 2009).

Several chlorophyll *a* fluorescence OJIP fast kinetics parameters, especially the PI and the RC/ABS, indicated significant differences between genotypes. These indicators are mostly used to monitor stress responses in tree species (Desotgiu et al., 2012). The higher energy conservation with the increased CO_2 assimilation rate can contribute to increases in biomass productivity in these autotetraploid plants. Higher (by 25%–30%) chlorophyll *a* and *b* contents in greenhouse-grown leaves (Table III) can reflect more efficient light utilization. Smaller differences in the chlorophyll contents between diploid and tetraploid plants were detectable under field conditions. Elevated levels of GAs and trans-zeatin measured in the field in the tetraploid willow plants can influence photosynthetic events, especially chloroplast functions. Jiang et al. (2012) analyzed the effects of the DELLA *gai1* mutation on chloroplast biogenesis and concluded that GAs indirectly promote chloroplast division through their impact on leaf mesophyll cell expansion. A close link between cytokinins and chloroplast differentiation has been reported repeatedly (for review, see Cortleven and Schmülling, 2015). Analytical studies on hormone contents of willow leaves identified salicylic acid as being significantly elevated after polyploidization (Table II). Salicylic acid can be involved in various steps of photosynthetic regulation (for review, see Rivas-San Vicente and Plasencia, 2011). Treatment of *Brassica juncea* plants with a low concentration (10^{-5} M) of salicylic acid resulted in higher net photosynthetic rate and carboxylation efficiency (Fariduddin et al., 2003).

Characteristic anatomical changes caused by autotetraploidy include the considerable increase in midrib size (Fig. 6). The structure of these major veins with their numerous xylem conduits may affect the water transport capacity. Taneda and Terashima (2012) reported coordination in the development of the midrib xylem and the leaf lamina area. In the case of tetraploid willow plants, these two traits were enlarged simultaneously. As shown in Table II, accumulation of abscisic acid in leaves was not influenced significantly by genome size alteration. Abscisic acid content seems to reflect predominantly the water relations in plants. Another stress hormone, jasmonic acid and its derivative, jasmonate-Ile, were detected in leaves of tetraploids at higher concentrations than in diploid leaves. Jasmonate-Ile is the active form of jasmonic acid in plants, functioning in defense against insects, microbial pathogens, and abiotic stresses (Browse, 2009).

The Autotetraploid Genome of Energy Willow Plants Regulates the Development of an Enlarged Root System

Results of the phenotypic characterization of autoploid tree species published previously have only been focused on aboveground traits (Blakesley et al., 2002;

Ewald et al., 2009; Tang et al., 2010; Cai and Kang, 2011; Harbard et al., 2012; Mu et al., 2012). This study extends this knowledge and shows substantial changes in the size and structure of roots developed by willow plants with $2n = 4x = 76$ chromosomes relative to diploids. As an outcome of intensified plant phenotyping research, several alternative methods exist for the nondestructive imaging of root systems grown in either soil-free medium or rhizotrons filled with soil (for review, see Walter et al., 2015). Differences in root biomass between genotypes were recorded already during the first weeks (Fig. 12B). After a longer growing period, the tetraploid genotypes produced significantly larger root biomass. The functions of root meristems including stem cells are under the control of a complex hormonal network that regulates the growth of the root system (for review, see Pacifici et al., 2015). Accordingly, the hormone data provided can support the interpretation of the increased root production in the tetraploid willow lines. Significant increases were detected in the levels of active cytokinins, indole-3-acetic acid, and salicylic acid in the root tips of the PP-E7 and PP-E13 genotypes (Table IV). Lack of correlation was reported between concentrations of GAs and root biomass. The GA-deficient (35S:*PcGA2ox1*) and GA-insensitive (35S:*rgl1*) transgenic *Populus* spp. plants developed larger root systems regardless of lower or higher GA contents in the root tissues (Gou et al., 2010). In semidwarf hybrid poplar with elevated GAs, root biomass was enhanced (Elias et al., 2012). Plants with an enlarged root system, carrying the tetraploid willow genotypes described, can be more efficient in reaching and extracting nutrients and water even under conditions of limited availability. These plants can also be used for the detoxification of contaminated soils. Both green and root biomass productivities determine the effectiveness of phytoremediation by tree species in removing heavy metals and organic contaminants from the environment (Marmiroli et al., 2011).

CONCLUSION

Artificial production of novel willow genotypes with autotetraploid genomes resulted in substantial modifications in the developmental program that can be valuable for wider use of this species as a short-rotation energy crop. The environmental impact of the increased CO_2 fixation and improved photosynthetic efficiency can attract special attention in attempts to reduce the negative impacts of climate change. Despite the fact that this work is focused on the early developmental phase of tetraploid willow plants, several of the described traits can play a role in wood productivity during the subsequent cultivation of these genotypes in the short-rotation system. Based on the observed morphological and physiological features of these new genotypes, the application of autopolyploidization as an old breeding technique with new potentials can gain increasing significance, especially in the improvement of vegetatively propagated woody species. Plants bred with this chromosome engineering technique are not considered as genetically modified organisms. This legal status opens large potentials even in countries or regions where the breeding and cultivation of transgenic crops are prohibited by law. The data presented here are consistent with several previously described characteristics of other autotetraploid woody plants, where duplication of the plant genome caused very complex, multiple changes at the anatomical and morphological levels and in growth parameters of aboveground organs. Furthermore, this work provides additional information about alterations in the hormonal status of leaves and root tips as well as the stimulation of root development. We propose a key role for the increased GA and cytokinin levels in controlling traits of autotetraploid woody plants. Importantly, our interpretation of new tetraploid phenotypes could frequently be based on results from studies of transgenic wood species. The tetraploid variants described can also serve as crossing partners with diploids in order to produce triploid genotypes, which have been shown to be the most productive genetic background in willow wood production (Serapiglia et al., 2014).

MATERIALS AND METHODS

In Vitro Polyploidization of Energy Willow

Salix viminalis var. Energo plantlets kindly provided by Ferenc Kósa and Miklós Ift (Kreátor) were propagated as in vitro sterile cultures with a one-half-strength concentration of hormone-free Murashige and Skoog medium (Murashige and Skoog, 1962). These cultures were maintained under continuous light. Shoot apical meristems of 8- to 10-cm plantlets were decapitated, and 48 h later, stem sections with axillary buds were placed into sterile colchicine solution (0.05% or 0.1% [w/v]) and incubated for 48 h in dark. After colchicine treatment, these stem sections were rinsed three times in sterile distilled water and placed on hormone-free 0.6% (w/v) agar medium without colchicine. Two- to 3-cm-long shoots grown from the treated axillary buds were cut and placed in agar-solidified culture medium and used for further in vitro propagation. The differentiated roots were used for ploidy analyses. During the years, the tetraploid plantlets were maintained and propagated by nodal cuttings in vitro, and 8- to 10-cm-high rooted plantlets were transferred to soil in the greenhouse. Under these conditions, these willow plants developed green woody stems that can be used as a propagation material for both greenhouse and field studies. Not all lines were available for each comparison, but all lines that were analyzed for a given comparison are shown in the corresponding figure.

Flow Cytometry

Root tips (approximately 5–10 mm) of 2-week-old cuttings were excised from the plants grown either in agar medium or in water used for rooting willow cuttings. Determination of ploidy levels was conducted by flow cytometry (BD FACSCalibur) equipped with a 532-nm green solid-state laser operating at 30 mW. Nuclei extractions were done by chopping 15 mg of root tips on ice with a razor blade in a 55-mm petri dish containing 1 mL of Galbraith's buffer (Galbraith et al., 1983; 0.2 M Tris-HCl, 45 mM $MgCl_2$, 30 mM sodium citrate, 20 mM 4-morpholinepropane sulfonate, and 1% [v/v] Triton X-100, pH 7) and then filtered through a 40-μm nylon mesh. The suspension of released nuclei was stained with 1 $\mu g\ mL^{-1}$ propidium iodide (Sigma) for 10 min. At least 5,000 gated particles were analyzed per sample. Identical instrument settings were used in order to have comparable relative fluorescence intensity values while analyzing diploid and tetraploid samples. To test the uniformity of ploidy levels, multiple stem cuttings were used for a given plant.

Chromosome Counting

For the determination of chromosome numbers in mitotic willow cells, the previously described protocol developed for energy willow was used (Németh et al., 2013). Briefly, the mitotic events were synchronized by cold treatment at 4°C for 4 d. After 22 h of incubation at room temperature, root tips were collected and fixed in Carnoy's solution (ethanol:acetic acid, 3:1 [v/v]). Cell walls of the fixed roots were digested in 1% enzyme mixture: 0.3% (w/v) cellulase, 0.3% (w/v) pectolyase, and 0.3% (w/v) cytohelicase, and squash preparations were made in 45% acetic acid. Glass slides were exposed to liquid nitrogen, and after removal of coverslips, cells were stained with DAPI and observed with an Olympus FV1000 confocal microscope.

Phenotyping of Shoot and Root Growth

As members of the European Plant Phenotyping Network, we have constructed a semiautomatic platform that was used previously for phenotyping aboveground organs of barley (*Hordeum vulgare*) and wheat (*Triticum aestivum*) plants (Cseri et al., 2013; Fehér-Juhász et al., 2014). Single dormant stem cuttings were planted into radio-tagged plexiglass columns with a mixture of 80% Terra peat soil and 20% sandy soil. Five plexiglass columns surrounded with polyvinyl chloride tubing were placed on a metal rack. Three racks were used for each genotype with random arrangement. Only the shoot-forming cuttings and healthy shoots were included in the analyses. The racks were rearranged every week after each imaging during the experiments. The level of illumination in the greenhouse was approximately 400 μmol photons m^{-2} s^{-1}. This level was fairly constant during the whole illumination period. Watering and digital imaging were performed once per week. Shoots developed from dormant buds were photographed with an Olympus C-7070WZ digital camera from seven different side positions, produced by 51.4° step rotation of the pot. Plant-related pixels were determined by separating the pot and background from the plant in each photograph using an in house-developed image-analysis software tool. The shoot and leaf surface that corresponds to the plant-related pixel number was provided as the average of green pixel counts derived from photographs of seven projections to minimize the variations in superposition of leaves and shoots.

In the case of roots, the plexiglass columns were photographed from four different side positions and from the bottom. The root-related white pixels were identified by subtracting the black soil background from the images. Pixel numbers were converted to millimeters using 65-mm diameter pots captured in the images. To characterize the root area appearing at the surface of the chamber, the metric values of the area of the four side view projections (90° rotation) are summarized and the metric value of the area of the bottom view is added.

After completion of a 7-week phenotyping experiment, the rooted stems were removed from the soil and the roots were separated from the soil. Root weights were measured immediately after removal from the soil (wet weight) or after air drying for 1 d at 21°C (dry weight) before weight determination.

For field analysis of early growth, we used second year shoots of plants from the stock collection that was established by planting willow plants grown in pots in the greenhouse in the soil of the experimental field in the spring (April). The unfertilized soil was cultivated by disc-harrow. Because of limitation in the available number of plants from different genotypes, these plants were placed in single rows 1 m apart. On average, five to six plants per genotype were used in field analyses. Plant density was 50 cm within rows. After the growing season, 1-year-old willow stems were cut off during the winter (January) to stimulate coppicing from the stools. The growth rate of newly developing shoots was measured to monitor both primary and secondary growth during an 8-d period at the end of April and the first days of May. During this period, the average daily temperature was 21.5°C and the average temperature at night was 9°C.

Leaf Parenchyma and Root Cortex Cell Size Determination

The youngest fully developed leaves were cut transversely at the middle of the leaf and fixed with 4% formaldehyde in phosphate-buffered saline with 0.5% Triton X-100 for 4 h at 23°C in a tube roller. After three 10-min washes, thin hand sections were prepared from the midpoint between the midrib and the border of leaves. Sections were mounted in 0.1 mg mL^{-1} Calcofluor White in water and imaged using confocal laser scanning microscopy. Perimeters of leaf parenchyma cells were manually traced in Olympus Fluoview software and plotted. Using the same software, the number of cells in 100 μm was also calculated and plotted using Microsoft Excel software. For each genotype, four leaves were collected from two different plants, and on more than 40 images, a total of 200 cells were scored for cross-sectional area measurements. For root cortex cell size measurements, stem cuttings were rooted in water for 2 weeks. Root samples excised from the maturation zone were fixed, stained, and imaged as in the case of leaf samples above. To eliminate the ambiguity of root cortex cell size at the boundary regions (close to the epidermis and near stele regions), the middle 50% of the cortical region was identified as a curved strip using Olympus Fluoview software, and all cells in this region (including cells touching the strip borders) were manually traced to calculate the average cross-sectional area of the midcortex cells. For each genotype, four roots were collected from two different plants, and on 12 nonconsecutive hand sections, a minimum of 362 cells was scored for root midcortex region cell cross-sectional area measurements.

Microscopy of Cells and Tissue Sections

Confocal laser scanning microscopy was performed using an Olympus Fluoview FV1000 laser scanning confocal microscope (Olympus Life Science Europa). The microscope configuration was as follows: objective lenses, UPLSAPO 10× (dry, numerical aperture 0.4), UPLSAPO 20× (dry, numerical aperture 0.75), and UPLFLN 40× (oil, numerical aperture 1.3); sampling speed, 4 μs $pixel^{-1}$; line averaging, 2×; scanning mode, unidirectional; excitation, 405 nm (for both DAPI and Calcofluor White); laser transmissivity, less than 10%; main dichroic beamsplitter, DM405/488/543; intermediate dichroic beamsplitter, SDM 490; blue emission was detected between 425 and 475 nm. Bright-field images were captured with the same laser line. For imaging hand-sectioned stem cross sections, an Olympus SZX12 stereomicroscope with 0.5× and 1× objectives was used. For white light illumination, a white light-emitting diode light source (Photonic Optics) in combination with transmission light mode was used. Photographss of stem sections were captured using an Olympus Camedia C7070 digital camera using DScaler software (version 4.1.15; http://deinterlace.sourceforge.net/). Composite images were prepared using CorelDraw Graphics Suite X7 (Corel).

Gas-Exchange Measurements

The gas-exchange parameters CO_2 uptake rate, transpiration, and stomatal conductance were measured using a Licor 6400 gas analyzer (LI-COR). Attached leaves of greenhouse-grown plants were inserted into the gas cuvette for the measurements. The gas cuvette conditions were set to 400 μl/L CO_2, ambient temperature, and growth light intensity of 400 to 450 μmol m^{-2} s^{-1} photosynthetic active radiation (Mulkey and Smith, 1988; Taiz and Zeiger, 2010).

ETR: Light Response Curves of PSI and PSII

The ETR through PSII [ETR(II) = 0.5 × Y(II) × PPFD × 0.84] as well as through PSI [ETR(I) = 0.5 × Y(I) × PPFD × 0.84] were simultaneously measured using the Dual PAM-100 system (Walz; Baker, 2008, Klughammer and Schreiber, 1994). The effective quantum yield of photochemical energy conversion in PSII was calculated as Y(II) = $(F_m' - F)/F_m'$ (Genty et al., 1989), where F_o and F_o' are dark fluorescence yields from dark- and light-adapted leaf, respectively, and F_m and F_m' are maximal fluorescence yields from dark- and light-adapted leaf, respectively. The photochemical quantum yield of PSI, Y(I), is the quantum yield of photochemical energy conversion. It is calculated as Y(I) = $(P_m' - P)/P_m$ (Klughammer and Schreiber, 1994). The $P700^+$ signals (P) may vary between a minimal (P700 fully reduced) and a maximal (P700 fully oxidized) level. The maximum level of $P700^+$ is called P_m in analogy with F_m. It was determined with application of a pulse (300 ms) of saturation light (10,000 μE, 635 nm) after preillumination with far-red light. P_m' is analogous to the fluorescence parameter F_m' and was determined by applying a saturation pulse on top of actinic illumination.

Chlorophyll *a* Fluorescence Fast Kinetics Measurements

OJIP chlorophyll *a* fluorescence transients were measured by a Plant Efficiency Analyzer (Pocket Pea; Hansatech). The transients were induced by red light from a light-emitting diode source (627 nm, up to 3,500 μmol m^{-2} s^{-1} intensity). Prior to measurements, the adaxial surface of the selected leaves was adapted to darkness for 20 min using light-tight leaf clips. The OJIP test (Strasser et al., 2000) was used to analyze the chlorophyll *a* fluorescence transients, and the following original data were acquired: O (F_o) initial fluorescence level (measured at 50 μs), P (F_m) maximal fluorescence intensity, as well as the

J (at about 2 ms) and the I (at about 30 ms) intermediate fluorescence levels. From these specific fluorescence features, the following parameters of photosynthetic efficiency were calculated: maximal PSII quantum yield, F_v/F_m; ratio of variable fluorescence to initial fluorescence, F_v/F_o, where $F_v = F_m - F_o$; probability of electron transport out of the primary electron-accepting plastoquinone of PSII $(1 - V_j)/V_j$, where $V_j = (F_{2ms} - F_o)/F_v$; total complementary area between the fluorescence induction curve and F_m of the OJIP curve, area; and amount of active reaction centers per absorption, RC/ABS (Żurek et al., 2014). The relative measurement of efficiency for electron transport, PI, was as follows (Zivcak et al., 2008):

$$PI_{abs} = \frac{1 - (F_o/F_m)}{M_o/V_j} \times \frac{F_m - F_o}{F_o} \times \frac{1 - V_j}{V_j}$$

where $M_o = 4 \times (F_{300\,\mu s} - F_o)/(F_m - F_o)$ represents the initial slope of fluorescence kinetics.

Chlorophyll and Total Carotenoid Content Estimation

Sampling was done on the sixth or seventh fully opened leaves from the top. Pigment extraction was done using dimethylformamide (Jacobsen et al., 2012). Leaf discs of 0.8 cm were immersed in 1 mL of dimethylformamide for 48 h. The spectral determination of chlorophylls *a* and *b*, as well as total carotenoids, was carried out according to Wellburn (1994): Car(x + c) $\mu g/cm^2$ = total leaf carotenoids [xanthophyll (x) plus carotenes (c)].

Analysis of Hormone Contents in Leaves and Root Tips

Leaf and root samples (50–100 mg fresh weight) were purified and analyzed according to Dobrev and Kamínek (2002) and Dobrev and Vanková (2012). Mixed samples of the youngest fully expanded leaves without the main vein or mixed samples of the root tips (approximately 5 mm) or elongation zones (15–25 mm from the tip) were homogenized with a ball mill (MM301; Retsch) and extracted in cold (−20°C) methanol:water:formic acid (15:4:1, v/v/v). The following labeled internal standards (10 pmol per sample) were added: [$^{13}C_6$]IAA (Cambridge Isotope Laboratories), [$^2H_4$]salicylic acid (Sigma-Aldrich), [$^2H_3$]phaseic acid (NRC-PBI), [$^2H_6$]abscisic acid, [$^2H_5$]trans-zeatin, [$^2H_5$]trans-ZR, [$^2H_5$]trans-Z7G, [$^2H_5$]trans-Z9G, [$^2H_5$]trans-ZOG, [$^2H_5$]trans-ZROG, [$^2H_5$]trans-ZRMP, [$^2H_3$]DHZ, [$^2H_3$]DHZR, [$^2H_3$]DHZ9G, [$^2H_6$]iP, [$^2H_6$]iPR, [$^2H_6$]iP7G, [$^2H_6$]iP9G, and [$^2H_6$]iPRMP (Olchemim). The extract was purified using an SPE-C18 column (SepPak-C18; Waters) and a mixed-mode reverse phase, cation-exchange SPE column (Oasis-MCX; Waters). Two hormone fractions were sequentially eluted: (1) fraction A, eluted with methanol, containing auxins, abscisic acid, salicylic acid, jasmonic acid, and GA; and (2) fraction B, eluted with 0.35 M NH_4OH in 60% methanol containing cytokinins. Hormone metabolites were analyzed using HPLC (Ultimate 3000; Dionex) coupled to a hybrid triple quadrupole/linear ion-trap mass spectrometer (3200 Q TRAP; Applied Biosystems). Quantification of hormones was done using the isotope dilution method with multilevel calibration curves ($r^2 > 0.99$). Data processing was carried out with Analyst 1.5 software (Applied Biosystems). Data are presented as means ± SE.

Statistical Analyses

For the statistical analyses, Welch's *t* test was used for pairwise comparisons between the traits of diploid and tetraploid samples. Welch's *t* test is an adaptation of Student's *t* test and is more reliable if the samples have unequal sample sizes or variances (Ruxton, 2006). Additionally, multiple comparison analyses were also performed using ANOVA followed by posthoc Tukey's HSD test. Apart from Figure 2A, there were statistically significant differences between group means. The family-wise significance level for Tukey's HSD test was set to a rather conservative value of 0.05 (Quinn and Keough, 2002), which granted an additional, more stringent level of significance threshold during comparison of tetraploids with diploids. Welch's *t* test significance levels are indicated with asterisks, which are underlined based on the results of Tukey's HSD test. In rare cases, *P* values calculated by Tukey's test fell into a higher significance interval as compared with *P* values obtained by *t* test. These cases are indicated with underlined periods in the tables. For all statistical analyses, R statistical analysis software was used (R Core Team; https://www.R-project.org/).

For all genotypes, the traits of individual plants were measured, and the distribution of data was displayed by box and whisker plots (Spitzer et al., 2014). The plots were generated with the Web tool BoxPlotR (http://boxplot.tyers lab.com/) and edited with CorelDraw Graphics Suite X7. For phenotyping studies, the data analysis was performed by an in house-developed software package based on Matlab software tools (version 2008b) with the Image Processing Toolbox (MathWorks).

In photosynthetic studies, the data were visualized and evaluated by the following methods: for ETR(I) and ETR(II) measurements, Dual PAM version 1.18 and Origin 2015; for gas-exchange measurements, LI-6400 OPEN Software version 5.3 and Origin 2015; for chlorophyll fluorescence parameters deduced from OJIP fast kinetics measurements, PEA Plus version 1.00 and Origin 2015. Spider graph values are displayed after normalization to respective values obtained in the diploid line.

ACKNOWLEDGMENTS

We thank Ferenc Kósa and Miklós Ift for the initial stock of the willow variety Energo, Attila Herman for construction of the root phenotyping instrument in the GOP project, Pál Ormos for providing greenhouse and field facilities, Edit Kotogány for flow cytometric analyses, and Zsuzsanna Kószó for technical contributions in microscopy.

Received October 30, 2015; accepted December 31, 2015; published January 15, 2016.

LITERATURE CITED

Alonso-Ramírez A, Rodríguez D, Reyes D, Jiménez JA, Nicolás G, López-Climent M, Gómez-Cadenas A, Nicolás C (2009) Evidence for a role of gibberellins in salicylic acid-modulated early plant responses to abiotic stress in Arabidopsis seeds. Plant Physiol **150:** 1335–1344

Baker NR (2008) Chlorophyll fluorescence: a probe of photosynthesis in vivo. Annu Rev Plant Biol **59:** 89–113

Barcaccia G, Meneghetti S, Albertini E, Triest L, Lucchin M (2003) Linkage mapping in tetraploid willows: segregation of molecular markers and estimation of linkage phases support an allotetraploid structure for *Salix alba* × *Salix fragilis* interspecific hybrids. Heredity (Edinb) **90:** 169–180

Blakesley D, Allen A, Pellny TK, Roberts AV (2002) Natural and induced polyploidy in *Acacia dealbata* Link. and *Acacia mangium* Willd. Ann Bot (Lond) **90:** 391–398

Browse J (2009) Jasmonate passes muster: a receptor and targets for the defense hormone. Annu Rev Plant Biol **60:** 183–205

Cai X, Kang XY (2011) In vitro tetraploid induction from leaf explants of *Populus pseudo-simonii* Kitag. Plant Cell Rep **30:** 1771–1778

Camarero JJ, Palacio S, Montserrat-Martí G (2013) Contrasting seasonal overlaps between primary and secondary growth are linked to wood anatomy in Mediterranean sub-shrubs. Plant Biol (Stuttg) **15:** 798–807

Coate JE, Luciano AK, Seralathan V, Minchew KJ, Owens TG, Doyle JJ (2012) Anatomical, biochemical, and photosynthetic responses to recent allopolyploidy in Glycine dolichocarpa (Fabaceae). Am J Bot **99:** 55–67

Cortleven A, Schmülling T (2015) Regulation of chloroplast development and function by cytokinin. J Exp Bot **66:** 4999–5013

Cseri A, Sass L, Törjék O, Pauk J, Vass I, Dudits D (2013) Monitoring drought responses of barley genotypes with semi-robotic phenotyping platform and association analysis between recorded traits and allelic variants of some stress genes. Aust J Crop Sci **7:** 1560–1570

Cunniff J, Cerasuolo M (2011) Lighting the way to willow biomass production. J Sci Food Agric **91:** 1733–1736

De Lojo J, Di Benedetto A (2014) Biomass accumulation and leaf shape can be modulated by an exogenous spray of 6-benzylaminopurine in the ornamental foliage plant, *Monstera deliciosa* (Liebm.). J Hortic Sci Biotechnol **89:** 136–140

Desotgiu R, Pollastrini M, Cascio C, Gerosa G, Marzuoli R, Bussotti F (2012) Chlorophyll *a* fluorescence analysis along a vertical gradient of the crown in a poplar (Oxford clone) subjected to ozone and water stress. Tree Physiol **32:** 976–986

Didi V, Jackson P, Hejátko J (2015) Hormonal regulation of secondary cell wall formation. J Exp Bot **66:** 5015–5027

Dobrev PI, Kamínek M (2002) Fast and efficient separation of cytokinins from auxin and abscisic acid and their purification using mixed-mode solid-phase extraction. J Chromatogr A **950:** 21–29

Dobrev PI, Vanková R (2012) Quantification of abscisic acid, cytokinin, and auxin content in salt-stressed plant tissues. Methods Mol Biol **913:** 251–261

Dorn RD (1976) A synopsis of American Salix. Can J Bot **54:** 2769–2789
Dubouzet JG, Strabala TJ, Wagner A (2013) Potential transgenic routes to increase tree biomass. Plant Sci **212:** 72–101
Elias AA, Busov VB, Kosola KR, Ma C, Etherington E, Shevchenko O, Gandhi H, Pearce DW, Rood SB, Strauss SH (2012) Green revolution trees: semidwarfism transgenes modify gibberellins, promote root growth, enhance morphological diversity, and reduce competitiveness in hybrid poplar. Plant Physiol **160:** 1130–1144
Eriksson ME, Israelsson M, Olsson O, Moritz T (2000) Increased gibberellin biosynthesis in transgenic trees promotes growth, biomass production and xylem fiber length. Nat Biotechnol **18:** 784–788
Ewald D, Ulrich K, Naujoks G, Schöder MB (2009) Induction of tetraploid poplar and black locust plants using colchicine: chloroplast number as an early marker for selecting polyploids in vitro. Plant Cell Tissue Organ Cult **99:** 353–357
Fariduddin Q, Hayat S, Ahmad A (2003) Salicylic acid influences net photosynthetic rate, carboxylation efficiency, nitrate reductase activity, and seed yield in *Brassica juncea*. Photosynthetica **41:** 281–284
Fehér-Juhász E, Majer P, Sass L, Lantos C, Csiszár L, Turóczy Z, Mihály R, Mai A, Horváth GV, Vass I, et al (2014) Phenotyping shows improved physiological traits and seed yield of transgenic wheat plants expressing the alfalfa aldose reductase under permanent drought stress. Acta Physiol Plant **36:** 663–673
Galbraith DW, Harkins KR, Maddox JM, Ayres NM, Sharma DP, Firoozabady E (1983) Rapid flow cytometric analysis of the cell cycle in intact plant tissues. Science **220:** 1049–1051
Genty B, Briantais JM, Baker NR (1989) The relationship between the quantum yield of photosynthetic electron transport and quenching of chlorophyll fluorescence. Biochim Biophys Acta **990:** 87–92
Golzarian MR, Frick RA, Rajendran K, Berger B, Roy S, Tester M, Lun DS (2011) Accurate inference of shoot biomass from high-throughput images of cereal plants. Plant Methods **7:** 2
Gou J, Ma C, Kadmiel M, Gai Y, Strauss S, Jiang X, Busov V (2011) Tissue-specific expression of Populus C19 GA 2-oxidases differentially regulate above- and below-ground biomass growth through control of bioactive GA concentrations. New Phytol **192:** 626–639
Gou J, Strauss SH, Tsai CJ, Fang K, Chen Y, Jiang X, Busov VB (2010) Gibberellins regulate lateral root formation in Populus through interactions with auxin and other hormones. Plant Cell **22:** 623–639
Griffin AR, Chi NQ, Harbard JL, Son DH, Harwood CE, Price A, Vuong TD, Koutoulis A, Thinh HH (2015) Breeding polyploid varieties of tropical acacias: progress and prospects. Southern Forests **77:** 41–50
Harbard JL, Griffin AR, Foster S, Brooker C, Kha LD, Koutoulis A (2012) Production of colchicine-induced autotetraploids as a basis for sterility breeding in *Acacia mangium* Willd. Forestry **85:** 3427–3436
Hartmann A, Czauderna T, Hoffmann R, Stein N, Schreiber F (2011) HTPheno: an image analysis pipeline for high-throughput plant phenotyping. BMC Bioinformatics **12:** 148
Huang JG, Deslauriers A, Rossi S (2014) Xylem formation can be modeled statistically as a function of primary growth and cambium activity. New Phytol **203:** 831–841
Jacobsen SE, Rosenqvist E, Bendevis M (2012) Chlorophyll extraction with dimethylformamide DMF. PrometheusWiki. http://prometheuswiki.publish.csiro.au/tikicitation.php?page=Chlorophyll%20extraction%20with%20Dimethylformamide%20DMF (August 13, 2015)
Jiang X, Li H, Wang T, Peng C, Wang H, Wu H, Wang X (2012) Gibberellin indirectly promotes chloroplast biogenesis as a means to maintain the chloroplast population of expanded cells. Plant J **72:** 768–780
Karp A, Hanley SJ, Trybush SO, Macalpine W, Pei M, Shield I (2011) Genetic improvement of willow for bioenergy and biofuels. J Integr Plant Biol **53:** 151–165
Klughammer C, Schreiber U (1994) An improved method, using saturating light pulses, for the determination of photosystem I quantum yield via $P700^+$-absorbance changes at 830 nm. Planta **192:** 261–268
Kubota HF, Yoshimura Y (2002) Estimation of photosynthetic activity from the electron transport rate of photosystem 2 in film-sealed leaf of sweet potato, *Ipomoea batatas* Lam. Photosynthetica **40:** 337–341
Li WD, Biswas DK, Xu H, Xu CQ, Wang XZ, Liu JK, Jiang GM (2009) Photosynthetic responses to chromosome doubling in relation to leaf anatomy in *Lonicera japonica* subjected to water stress. Funct Plant Biol **36:** 783–792
Licausi F, Ohme-Takagi M, Perata P (2013) APETALA2/Ethylene Responsive Factor (AP2/ERF) transcription factors: mediators of stress responses and developmental programs. New Phytol **199:** 639–649
Lu S, Lu X, Zhao W, Liu Y, Wang Z, Omasa K (2015) Comparing vegetation indices for remote chlorophyll measurement of white poplar and Chinese elm leaves with different adaxial and abaxial surfaces. J Exp Bot **66:** 5625–5637
Marmiroli M, Pietrini F, Maestri E, Zacchini M, Marmiroli N, Massacci A (2011) Growth, physiological and molecular traits in Salicaceae trees investigated for phytoremediation of heavy metals and organics. Tree Physiol **31:** 1319–1334
Matsumoto-Kitano M, Kusumoto T, Tarkowski P, Kinoshita-Tsujimura K, Václavíková K, Miyawaki K, Kakimoto T (2008) Cytokinins are central regulators of cambial activity. Proc Natl Acad Sci USA **105:** 20027–20031
Mu HZ, Liu ZJ, Lin L, Li HY, Jiang J, Liu GF (2012) Transcriptomic analysis of phenotypic changes in birch (*Betula platyphylla*) autotetraploids. Int J Mol Sci **13:** 13012–13029
Mulkey SS, Smith M (1988) Measurement of photosynthesis by infra red gas analysis. *In* CT Lange ed, Bioinstrumentation. American Biology Teachers Association, Warrenton, VA, pp 79–84
Murashige T, Skoog F (1962) A revised medium for rapid growth and bioassays with tobacco tissue cultures. Physiol Plant **15:** 473–497
Nelissen H, Rymen B, Jikumaru Y, Demuynck K, Van Lijsebettens M, Kamiya Y, Inzé D, Beemster GTS (2012) A local maximum in gibberellin levels regulates maize leaf growth by spatial control of cell division. Curr Biol **22:** 1183–1187
Németh AV, Dudits D, Molnár-Láng M, Linc G (2013) Molecular cytogenetic characterisation of *Salix viminalis* L. using repetitive DNA sequences. J Appl Genet **54:** 265–269
Newsholme C (1992) Willows, the *Genus Salix*. Timber Press, Portland, OR
Ohashi-Ito K, Saegusa M, Iwamoto K, Oda Y, Katayama H, Kojima M, Sakakibara H, Fukuda H (2014) A bHLH complex activates vascular cell division via cytokinin action in root apical meristem. Curr Biol **24:** 2053–2058
Pacifici E, Polverari L, Sabatini S (2015) Plant hormone cross-talk: the pivot of root growth. J Exp Bot **66:** 1113–1121
Quinn GP, Keough MJ (2002) Experimental Design and Data Analysis for Biologists. Cambridge University Press, Cambridge, UK, p 49
Rao G, Sui J, Zeng Y, He C, Zhang J (2015) Genome-wide analysis of the AP2/ERF gene family in *Salix arbutifolia*. FEBS Open Bio **5:** 132–137
Rivas-San Vicente M, Plasencia J (2011) Salicylic acid beyond defence: its role in plant growth and development. J Exp Bot **62:** 3321–3338
Ruxton GD (2006) The unequal variance t-test is an underused alternative to Student's t-test and the Mann–Whitney U test. Behav Ecol **17:** 688–690
Růžička K, Ursache R, Hejátko J, Helariutta Y (2015) Xylem development: from the cradle to the grave. New Phytol **207:** 519–535
Särkilahti E, Valanne T (1990) Induced polyploid in Betula. Silva Fennica **24:** 227–234
Serapiglia MJ, Gouker FE, Smart LB (2014) Early selection of novel triploid hybrids of shrub willow with improved biomass yield relative to diploids. BMC Plant Biol **14:** 74–86
Spitzer M, Wildenhain J, Rappsilber J, Tyers M (2014) BoxPlotR: a web tool for generation of box plots. Nat Methods **11:** 121–122
Strasser RJ, Srivastava A, Tsimilli-Michael M (2000) The fluorescence transient as a tool to characterize and screen photosynthetic samples. *In* M Yunus, UV Pathre, eds, Probing Photosynthesis: Mechanisms Regulation and Adaptation. Taylor & Francis, New York, pp 443–480
Strasser RJ, Tsimilli-Michael M, Srivastava A (2004) Analysis of the fluorescence transient. *In* GC Papageorgiou, Govindjee, eds, Chlorophyll Fluorescence: a Signature of Photosynthesis. Advances in Photosynthesis and Respiration Series. Springer, Dordrecht, The Netherlands, pp 321–362
Suda Y, Argus GV (1968) Chromosome numbers of some North American Salix. Brittonia **20:** 191–197
Sugiyama S (2005) Polyploidy and cellular mechanisms changing leaf size: comparison of diploid and autotetraploid populations in two species of Lolium. Ann Bot (Lond) **96:** 931–938
Tackenberg O (2007) A new method for non-destructive measurement of biomass, growth rates, vertical biomass distribution and dry matter content based on digital image analysis. Ann Bot (Lond) **99:** 777–783
Taiz L, Zeiger E (2010) Plant Physiology, Ed 5. Sinauer Associates, Sunderland, MA

Taneda H, Terashima I (2012) Co-ordinated development of the leaf midrib xylem with the lamina in *Nicotiana tabacum*. Ann Bot (Lond) **110:** 35–45

Tang ZQ, Chen DL, Song ZJ, He YC, Cai DT (2010) In vitro induction and identification of tetraploid plants of *Paulownia tomentosa*. Plant Cell Tissue Organ Cult **102:** 213–220

Walter A, Liebisch F, Hund A (2015) Plant phenotyping: from bean weighing to image analysis. Plant Methods **11:** 14

Wang J, Shi L, Song S, Tian J, Kang X (2013a) Tetraploid production through zygotic chromosome doubling in Populus. Silva Fennica **47:** 932

Wang Z, Wang M, Liu L, Meng F (2013b) Physiological and proteomic responses of diploid and tetraploid black locust (*Robinia pseudoacacia* L.) subjected to salt stress. Int J Mol Sci **14:** 20299–20325

Warner DA, Edwards GE (1989) Effects of polyploidy on photosynthetic rates, photosynthetic enzymes, contents of DNA, chlorophyll, and sizes and numbers of photosynthetic cells in the C4 dicot *Atriplex confertifolia*. Plant Physiol **91:** 1143–1151

Warner DA, Edwards GE (1993) Effects of polyploidy on photosynthesis. Photosynth Res **35:** 135–147

Wellburn AR (1994) The spectral determination of chlorophylls *a* and *b*, as well as total carotenoids, using various solvents with spectrophotometers of different resolution. J Plant Physiol **144:** 307–313

Ye ZH, Zhong R (2015) Molecular control of wood formation in trees. J Exp Bot **66:** 4119–4131

Zivcak M, Brestic M, Olsovska K, Slamka P (2008) Performance index as a sensitive indicator of water stress in *Triticum aestivum* L. Plant Soil Environ **54:** 133–139

Żurek G, Rybka K, Pogrzeba M, Krzyżak J, Prokopiuk K (2014) Chlorophyll *a* fluorescence in evaluation of the effect of heavy metal soil contamination on perennial grasses. PLoS ONE **9:** e91475